UNIVERSITY OF THESSALY

SCHOOL OF ENGINEERING
DEPARTMENT OF MECHANICAL ENGINEERING

Numerical calculation of Stress concentration factors in shafts with shoulder fillet discontinuities and comparison with theoretical results.

By

Thodoris Karatzaferis

Submitted in partial fulfillment of the requirements for the degree of Diploma in Mechanical Engineering at the University of Thessaly

Volos, 2021

Approved by the committee on final Examination:

Advisor	Dr. Sotiria Chouliara, Lab Teaching Personnel, Department of Mechanical Engineering, University of Thessaly
Member	Dr. Nikolaos Aravas, Professor, Department of Mechanical Engineering, Aristotle University of Thessaly
Member	Dr. Alexis Kermanidis, Associate Professor, Department of Mechanical Engineering, University of Thessaly

Date Approved: [July 8, 2021]

Numerical calculation of Stress concentration factors in shafts with shoulder fillet discontinuities under tension and comparison with theoretical results.

Thodoris Karatzaferis

Department of Mechanical Engineering, University of Thessaly

Supervisor: Dr Sotiria Chouliara

Lab Teaching Personnel

Abstract

In a loaded structural member, near changes in the section, distributions of stress occur in which the peak stress reaches much larger magnitudes than does the average stress over the section. Therefore, stress concentration in structural members is a classic topic of mechanical engineering and it is strongly associated with machine elements such as shafts. This project refers to shafts with circular cross section and shoulder fillet geometry and this configuration is examined under tension. Shafts, axles, spindles, rotors, and so forth, usually involve a number of diameters connected by shoulders with rounded fillets replacing the sharp corners. The purpose of this diploma thesis is the numerical study of stress concentration factors (SFC) in shafts with geometrical discontinuities and the comparison with previously reported theoretical results. Finite elements methods (ABAQUS) are applied to determine the corresponding stress concentration factors considering various parameters and then the numerical results are compared with theoretical results available in literature.

Contents

Chapter 1

1.1 Introduction

The first topic that should be discussed for this study is the definition of a shaft. A shaft is a rotating member, usually of circular cross section, used to transmit power or motion. It provides, the axis of rotation, or oscillation, of elements such as gears, pulleys, flywheels, cranks, sprockets, and the like and controls the geometry of their motion.

The main difference between a shaft and an axle is that the axle carries no torque, and it is used to support rotating wheels, pulleys, and the like. Both axles and shafts may not be uniform in their entire length. Shafts can be machined in order to be shaped into the desired shape. They can also obtain gradations in their diameter, to form wedges for fitting sprockets, pulleys and gears or even cutting on them gears or cams and thus form an integral part. Thus, the strain of the shafts corresponds to a complex load and is very difficult to be determined. Any shaft configuration that causes notches on the surface results in stress concentration in this area. When calculating the shafts in dynamic but also in static loading, this parameter is particularly important and must be considered.

In deciding on an approach to shaft sizing, it is necessary to realize that a stress analysis at a specific point on a shaft can be made using only the shaft geometry in the vicinity of that point. Thus, the geometry of the entire shaft is not needed. In design it is usually possible to locate the critical areas, size these to meet the strength requirements, and then size the rest of the shaft to meet the requirements of the shaft-supported elements.

The deflection and slope analyses cannot be made until the geometry of the entire shaft has been defined. Thus, deflection is a function of the geometry everywhere, whereas the stress at a section of interest is a function of local geometry. For this reason, shaft design allows a consideration of stress first. Then, after tentative values for the shaft dimensions have been established, the determination of the deflections and slopes can be made (Figure 1).

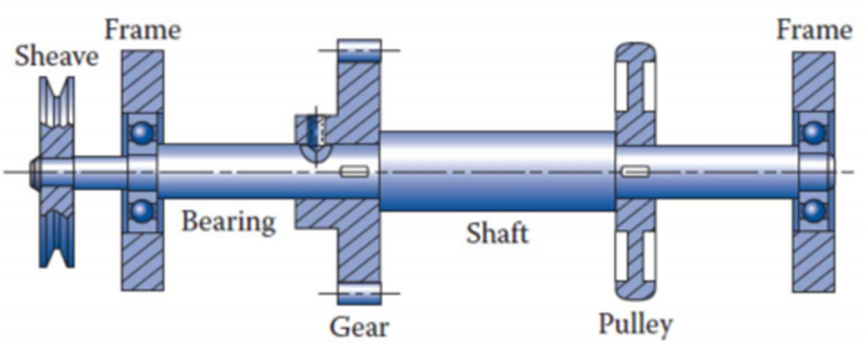

Figure 1 A stepped shaft with various elements attached.

1.2 Shafts Layout

The general layout of a shaft to accommodate machine elements such as gears, bearings, and pulleys, must be specified early in the design process in order to perform a free body force analysis and to obtain shear-moment diagrams. The geometry of a shaft is generally that of a stepped cylinder. The use of shaft shoulders is an excellent means of axially locating the shaft elements, so that they can carry any thrust loads. Each shoulder in the shaft serves a specific purpose, which is determined by observation.

The geometric configuration of a shaft to be designed is often simply a revision of existing models in which a limited number of changes can be made. If there is no existing design to use as a starter, the determination of the shaft layout may have many solutions. This problem is illustrated by the two examples of Figure 2. In Figure 2-a a geared countershaft is to be supported by two bearings. In Figure 2-c a fanshaft is to be configured.

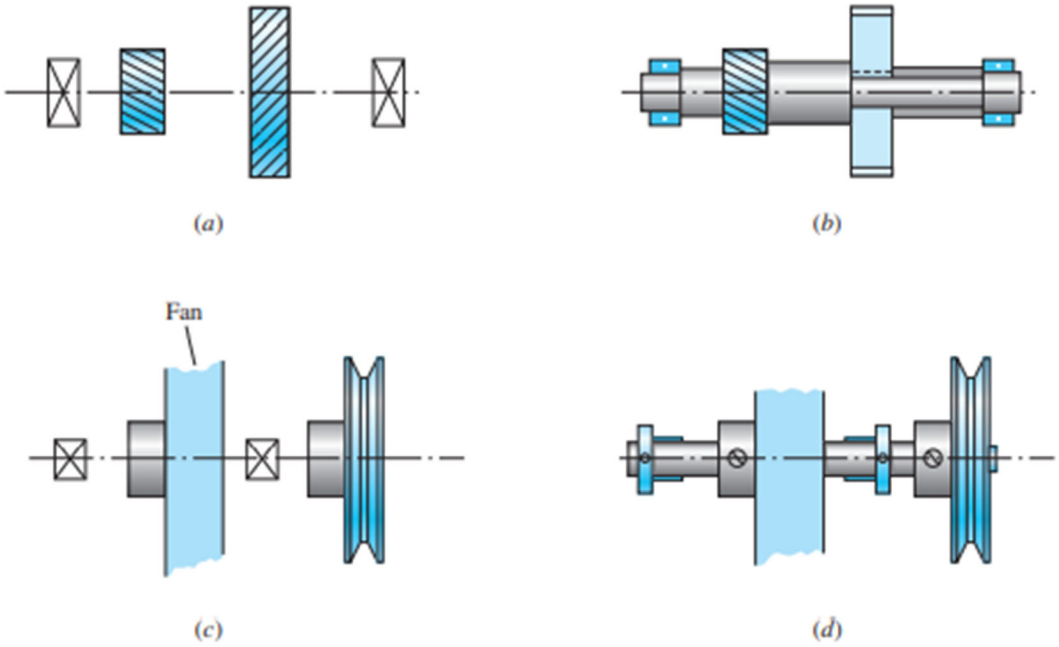

Figure 2 Shafts layouts and shaft-mounted devices.[1]

The solutions are shown in Figure 2-b and Figure 2-d are not necessarily the best ones, but they do illustrate how the shaft-mounted devices are fixed and located in the axial direction, and how provision is made for torque transfer from one element to another. There are no absolute rules for specifying the general layout, but the following guidelines may be helpful.

1.3 Shafts Materials

The necessary strength to resist loading stresses affects the choice of materials and their treatments. Many shafts are made from low carbon, cold-drawn or hot-rolled steel such as AISI 1020-1050 steels. The AISI 1020-1050 strength characteristics are given below by Table 1 [1].

Significant strengthening from heat treatment and high alloy content are often not warranted. Fatigue failure is reduced moderately by increase in strength, and then only to a certain level before adverse effects in endurance limit and notch sensitivity begin to counteract the benefits of higher strength. A good practice is a preliminary choice with inexpensive, low or medium carbon steel for the initial time through the design calculations. If strength considerations turn out to dominate over deflection, then a higher strength material should be tried, allowing the shaft sizes to be reduced until excess deflection

becomes an issue. The cost of the material and its processing must be weighed against the need for smaller shaft diameters. When warranted, typical alloy steels for heat treatment include AISI 1340-50, 3140-50, 4140, 4340, 5140, and 8650. Shafts usually do not need to be surface hardened unless they serve as the actual journal of a bearing surface. Typical material choices for surface hardening include carburizing grades of AISI 1020, 4320, 4820, and 8620.

1 UNS No.	2 SAE and/or AISI No.	3 Process-ing	4 Tensile Strength, MPa (kpsi)	5 Yield Strength, MPa (kpsi)
G10200	1020	HR	380 (55)	210 (30)
		CD	470 (68)	390 (57)
G10300	1030	HR	470 (68)	260 (37.5)
		CD	520 (76)	440 (64)
G10350	1035	HR	500 (72)	270 (39.5)
		CD	550 (80)	460 (67)
G10400	1040	HR	520 (76)	290 (42)
		CD	590 (85)	490 (71)
G10450	1045	HR	570 (82)	310 (45)
		CD	630 (91)	530 (77)
G10500	1050	HR	620 (90)	340 (49.5)

Table 1 Deterministic ASTM Minimum Tensile and Yield Strengths for Some Hot-Rolled (HR) and Cold-Drawn (CD) Steels.[1]

Cold drawn steel is usually used for diameters under about 3 inches. The nominal diameter of the bar can be left unmachined in areas that do not require fitting of components. Hot rolled steel should be machined all over. For large shafts requiring much material removal, the residual stresses may tend to cause warping. If concentricity is important, it may be necessary to rough machine, then heat treat to remove residual stresses and increase the strength, then finish machine to the final dimensions. In approaching material selection, the amount to be produced is a salient factor. For low production, turning is the usual primary shaping process.

An economic viewpoint may require removing the least material. High production may permit a volume conservative shaping method (hot or cold forming, casting), and minimum material in the shaft can become a design goal. Cast iron may be specified if the production quantity is high, and the gears are to be integrally cast with the shaft.

Properties of the shaft locally depend on its history-cold work, cold forming, rolling of fillet features, heat treatment, including quenching medium, agitation, and tempering regimen. Stainless steel may be appropriate for some environments[1].

1.4 Shoulder Fillets

The shoulder fillet (Figure 3) is the type of stress concentration that is more frequently encountered in machine design practice than any other. Shafts, axles, spindles, rotors, and so forth, usually involve a number of diameters connected by shoulders with rounded fillets replacing the sharp corners that were often used in former years. The best known summary of results for various geometric shapes is the work by Peterson [2] and is based on results from photoelastic testing.

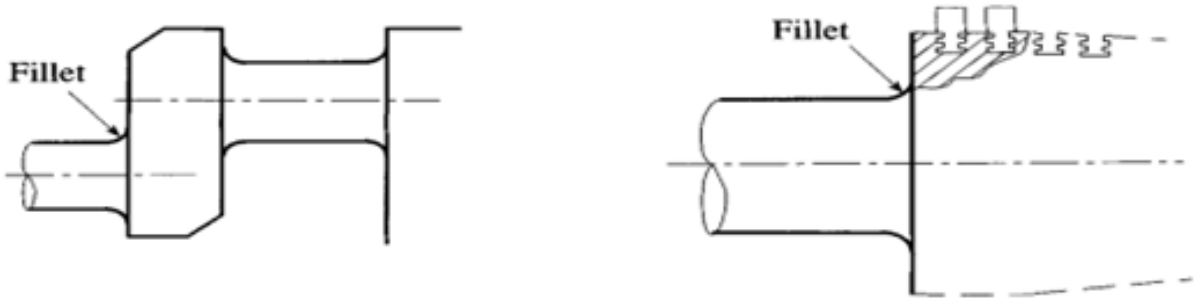

(a) (b)

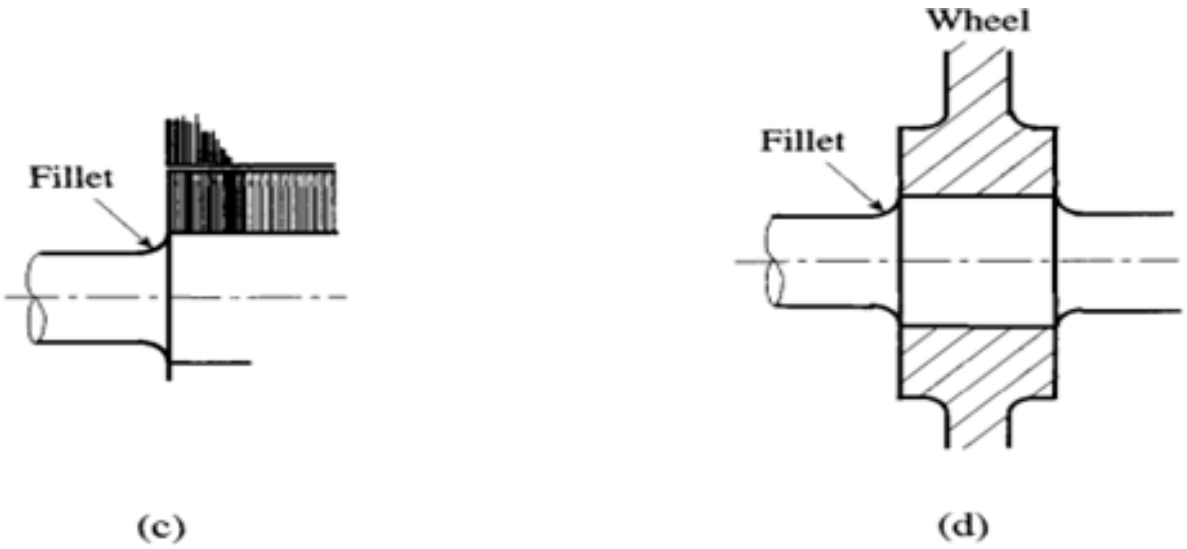

Figure 3 Examples of filleted members: (a) Engine crankshaft: (b) turbine rotor: (c) motor shaft: (d) railway axle.[2]

1.5 Shafts Design for Stress

The evaluation of the stress in shafts is the main concern of a mechanical engineer. Critical locations should be identified in order to avoid the stress concentration factors. The locations which are prone to high stresses and therefore to failure (static or dynamic), usually appear on the outer surface at axial locations where the bending moment is large, and the torque is present. The best way to design a shaft is to adopt a stress analysis (instead of a deflections analysis) and to compare various point among the shaft in order to identify the most critical locations.

Most shafts transmit torque through a portion of their length. Typically, the torque comes into the shaft at one gear and leaves the shaft at another gear. A free body diagram of the shaft allows the torque at any section to be determined. The torque is often relatively constant at steady state operation. The shear stress due to the torsion takes its maximum values on outer surfaces.

The ‘‘equivalent’’ moments on a shaft can be determined by shear and bending moment diagrams [7]. Since most shaft problems incorporate gears or pulleys that introduce forces in two planes, the shear and bending moment diagrams will generally be needed in two planes. Resultant moments are obtained by summing moments as vectors at points of interest along the shaft. The phase angle of the moments is not important since the shaft rotates, and this

makes the problem a ‘‘fully-reversed’’ load case. This term means that a steady bending moment will produce a completely reversed moment on a rotating shaft, as a specific stress element will alternate from compression to tension in every revolution of the shaft. The normal stress due to bending moments will be greatest on the outer surfaces. In situations where a bearing is located at the end of the shaft, stresses near the bearing are often not critical since the bending moment is small.

Axial stresses on shafts due to the axial components transmitted through helical gears or tapered roller bearings will almost always be negligibly small compared to the bending moment stress. They are often also constant, so they contribute little to fatigue. Consequently, it is usually acceptable to neglect the axial stresses induced by the gears and bearings when bending is present in a shaft. If an axial load is applied to the shaft in some other way, it is not safe to assume it is negligible without checking magnitudes.

1.6 Shaft Stresses

Bending, torsion and axial stress may be present together in both midrange and alternating components. For analysis the stresses, it is simply enough to combine the different types of stresses by Von Mises. Axial loads are usually very small at critical locations, because bending and torsion are dominate, so they are not taken into consideration. The stresses duo to bending and torsion are given by:

$$\sigma_{\alpha} = K_f \frac{M_a c}{I} \qquad \text{Eq. 1} \qquad \sigma_m = K_f \frac{M_m c}{I} \qquad \text{Eq. 3}$$

$$\tau_{\alpha} = \mathrm{K}_{fs} \frac{T_a r}{J} \qquad \text{Eq. 2} \qquad \tau_m = \mathrm{K}_{fs} \frac{T_m r}{J} \qquad \text{Eq. 4}$$

where M_m and M_a are the midrange and alternating bending moments, T_m and T_a are the midrange and alternating torques, and K_f and K_{fs} are the fatigue stress-concentration factors for bending and torsion, respectively.[1]

1.7 Sfafts Failures

There are four basic failure mechanisms: corrosion, wear, overload, and fatigue. The first two, corrosion and wear, almost never cause machine-shaft failures and, on the rare occasions they do, leave clear evidence. Of the other two mechanisms, fatigue is more common than overload failure.

- Overload failures

  Overload failures are caused by forces that exceed the yield strength or the tensile strength of a material. The appearance of an overload failure depends on whether the shaft material is brittle or ductile. No shaft materials are brittle or ductile. The shafts used on almost all motors, reducers and fans are low or medium carbon steels and relatively ductile. As a result, when an extreme overload is placed on these materials, they twist and distort. The bent shaft shown in Figure 4-a has been grossly overloaded by a torsional stress.

  There are occasional cases when a ductile shaft will fail in a somewhat brittle manner. Figure 4-b, shows an example of this situation, what happened when a 200 hp, 3600 RPM motor suddenly stopped running. The result was a huge torsional stress and a cracked shaft. But because the material is ductile, the angle of the crack it is not at the 45° position, and there is obvious distortion of the keyway. When ductile materials are grossly overloaded very rapidly, they tend to act in a brittle manner.

Figure 4 (a) Overloaded shaft by a torsional stress, (b) Brittle failure on a ductile shaft.

- Fatigue failure

Fatigue is caused by cyclical stresses, and the forces that cause fatigue failures are substantially less than those that would cause plastic deformation. Confusing the situation even further is the fact that corrosion will reduce the fatigue strength of a material. The amount of reduction is dependent on both the severity of the corrosion and the number of stress cycles.

Once they are visible to the naked eye, cracks always grow perpendicular to the plane of maximum stress. Figure 5 shows the fracture planes caused by four common fatigue forces. Because the section properties will change as the crack grows, it is crucial for the analyst to look carefully at the point where the failure starts to determine the direction of the forces. For example, while it is common for torsional fatigue forces to initiate a failure, the majority of the crack propagation could be in tension. That is because the shaft has been weakened and the torsional resonant frequency has changed.

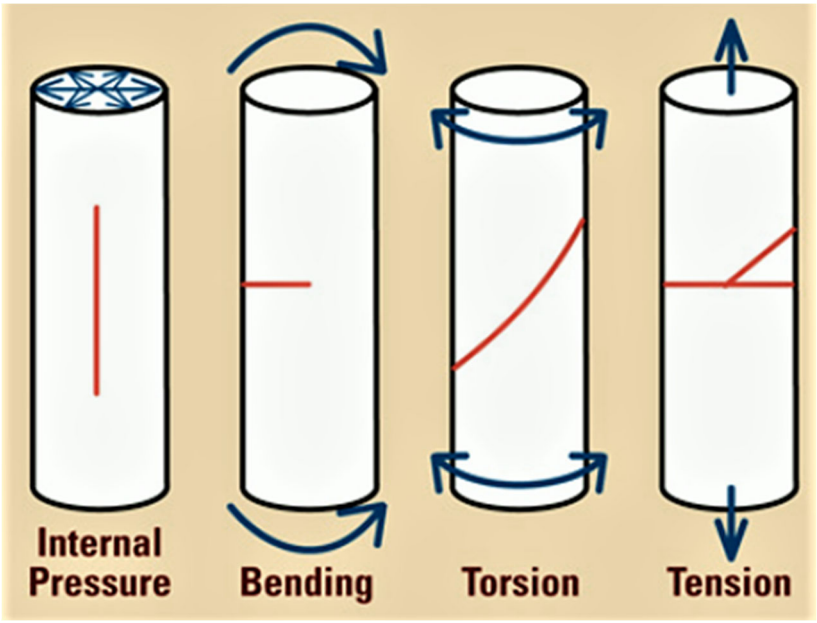

Figure 5 fracture planes caused by four common fatigue forces.

The condition or roughness of the fracture surface is one of the most important points to look at in analyzing a failure because of the difference between overload failures and fatigue failures. With overload failures, because the crack travels at a constant rate, the surface is uniformly rough. Fatigue induced cracks, however, travel

across the fracture face at ever-increasing speeds. As a result, the typical fatigue fracture face is relatively smooth near the origins and ends in a comparatively rough final fracture.

1.8 Stress Raisers

Most service failures in shafts are attributable largely to some condition that causes stress intensification. Locally, the stress value is raised above a value at which the material is capable of withstanding the number of loading cycles that corresponds to a satisfactory service life. Only one small area needs to be repeatedly stressed above the fatigue strength of the material for a crack to be initiated. An apparently insignificant imperfection such as a small surface irregularity may severely reduce the fatigue strength of a shaft if the stress level at the imperfection is high. The most vulnerable zone in torsional and bending fatigue is the shaft surface, an abrupt change of surface configuration may have a damaging effect, depending on the orientation of the discontinuity to the direction of stress.

Stress-raisers are sharp corners, grooves, notches, or acute changes of section that cause stress concentrations under normal loadings. As general rule, stress should be transmitted among the element without breaking some critical values and as smoothly as possible.

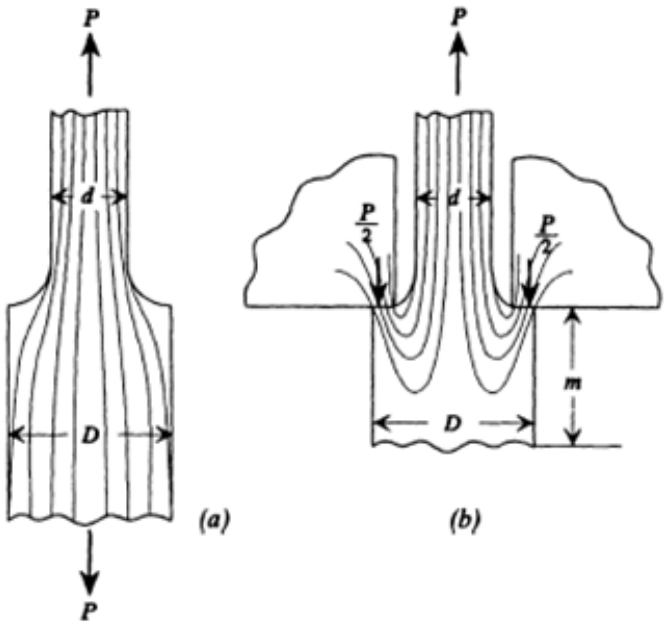

Figure 6 (*a*) Stress flow is smooth (*b*) Sharp change in the stress flow direction causes high stress.

Sharp transitions should be removed from the surface of the element in order to ensure a uniform stress flow. In the circumstances where the stress raisers are necessitated by the functional requirements, the geometrical discontinuities should be placed in areas where the nominal stress load in the minimum. In Figure 6 the stress flow is highly affected by the sharp changes of the geometry. Both parts have the same shape but totally different stress levels.

Another way to eliminate the stress raisers, in cases where the are necessary, is to remove an amount of the material near the geometrical discontinuity. By this way, it is possible to restrict the stress concentration effects and this is shown below by Figure 7.

Figure 7 Adding a notch as in case (b) can reduce the stress concentrations effects of the corner of (a).

Chapter 2

2.1 Stress Concentration Factor

A stress concentration (often called stress raiser) is a location in an object where stress is concentrated. The structure is strongest when force is evenly distributed over its area. Discontinuity in geometry, reduction in area or joint locations results in a localized increase in stress when subjected to external loading. The structure can fail due to such stress concentration when a concentrated stress exceeds the material's strength. The real fracture strength of a material is always lower than the theoretical value because most structural components or assemblies contain discontinuity in geometry or joints which induces stress concentration.

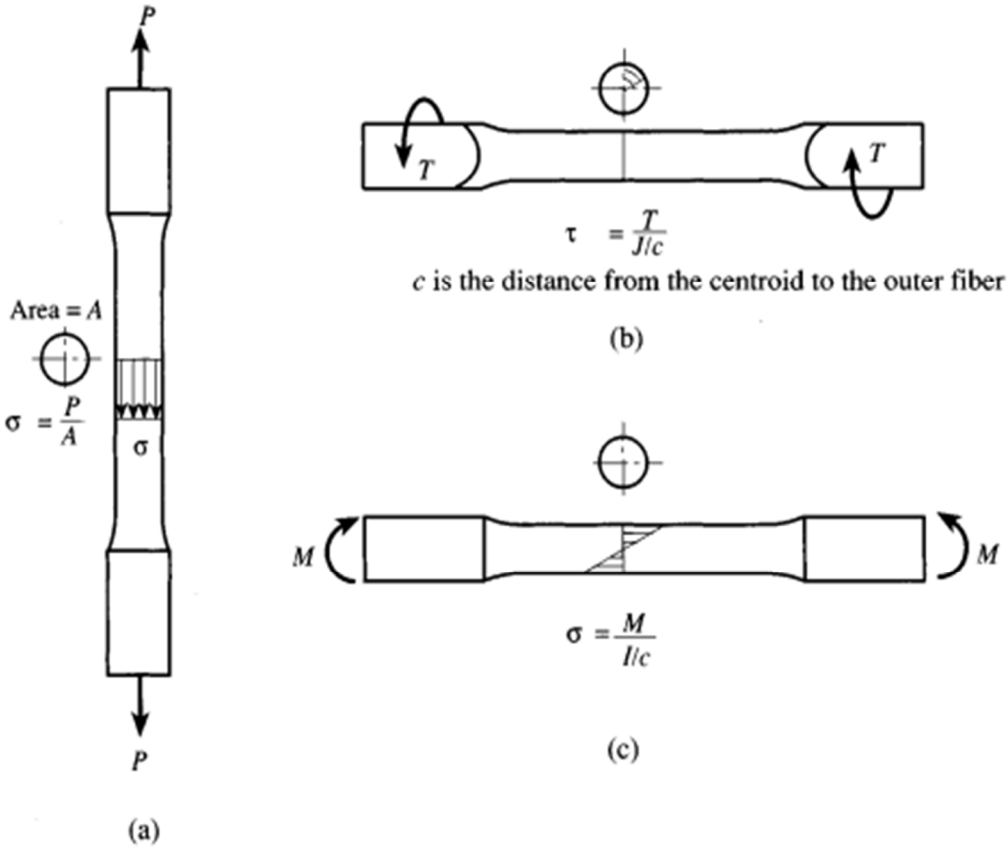

Figure 8 Elementary stress cases for specimens of constant cross section or with a gradual cross-sectional change (a) Tension (b) torsion (c) bending.[2]

Stress Concentration factors (K_t) for several simple geometrical discontinuities have been determined by researchers from experiments and analytical relations. Roark and Peterson [2] have compiled these into tabular (graphs) format. They also have been reproduced in a number of mechanical design texts and handbooks widely used.

Change in area of cross-section of stepped shaft results in stress concentration at the discontinuity. In order to reduce the effect of stress concentration at the region of change in cross-section, fillet of radius r is usually applied as shown in Figure 9.

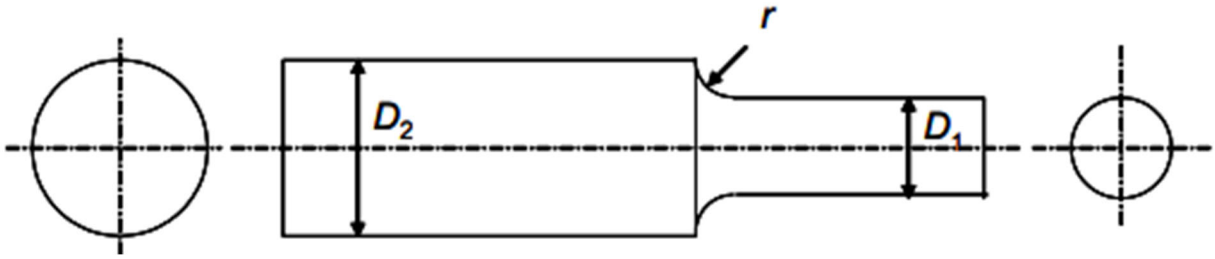

Figure 9 Circular stepped shaft with shoulder or radius r.

Thus, the magnitude of stress concentration factor is a function of non-dimensional parameter D_2 / D_1 and r / D_1. Stress concentration factor, K_t , can be written as:

$$\mathrm{K}_t = \frac{\sigma_{\max}}{\sigma_{nom}} \quad \text{for normal stress} \qquad \text{Eq. 5}$$

$$K_{ts} = \frac{\tau_{\max}}{\tau_{nom}} \quad \text{for shear stress} \qquad \text{Eq. 6}$$

The nominal stresses are given in Figure 8 for the different situations of stress load. Assuming a solid shaft with round cross section, appropriate geometry terms can be introduced for c, I, r, and J resulting in:

$$\sigma_{nom} = \frac{4P}{\pi D_1^{\,2}} \quad \text{for axial load} \qquad \text{Eq. 7}$$

$$\sigma_{nom} = \frac{32M}{\pi D_1^{\,3}} \quad \text{for bending load} \qquad \text{Eq. 8}$$

$$\tau_{nom} = \frac{16T}{\pi D_1^{\,3}} \quad \text{for tortion load} \qquad \text{Eq. 9}$$

2.3 Selection of Nominal Stresses

The definitions of the reference stresses σ_{nom} depend on the problem at hand. It is very important to properly identify the reference stress for the stress concentration factor of interest. The example below explains the selection of reference stress.

Example 1 Tension bar with a hole[2].

Uniform tension is applied to a bar with a single circular hole, as shown in Figure 10. The maximum stress occurs at point A, and the stress distribution can be shown to be as in Figure 10. The thickness of the plate is h, the width of the plate is H, and the diameter of the hole is d. The reference stress could be defined in two ways:

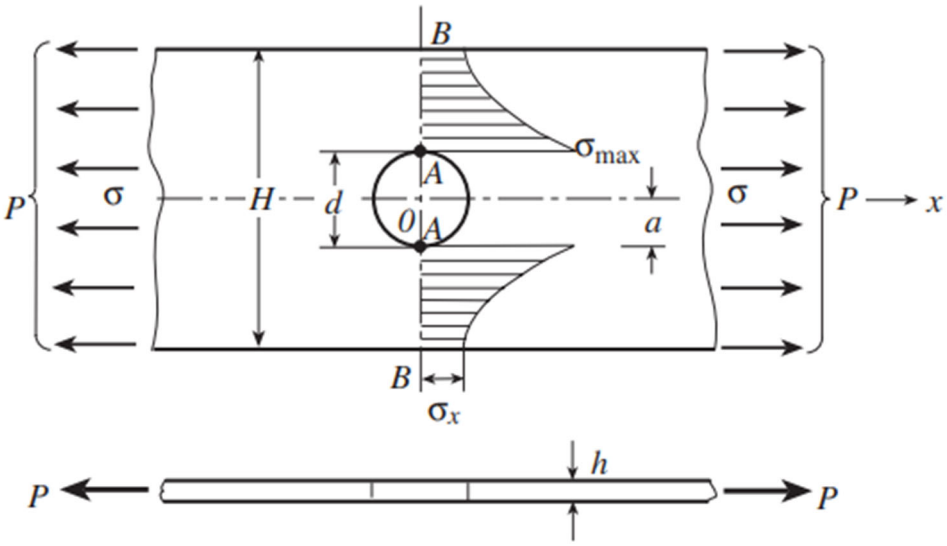

Figure 10 Tension bar with hole.[2]

a. The stress in a cross section far from the circular hole is called reference stress. The area at this section is called the gross cross-sectional area. Therefore:

$$\sigma_{nom} = \frac{P}{Hh} = \sigma \qquad \text{Eq. 10}$$

So that the stress concentration factor becomes:

$$K_{tg} = \frac{\sigma_{\max}}{\sigma_{nom}} = \frac{\sigma_{\max}}{\sigma} = \frac{\sigma_{\max} Hh}{P} \qquad \text{Eq. 11}$$

b. The stress based on the cross section at the hole, is formed by removing the circular hole from the gross cross section. The corresponding area is referred to as the net cross-sectional area. If the stresses at this cross section are uniformly distributed and equal to σ_n :

$$\sigma_n = \frac{P}{(H-d)h} \qquad \text{Eq. 12}$$

The stress concentration factor based on the reference stress σ_{nom} , namely, $\sigma_{nom} = \sigma_n$ is:

$$\mathrm{K}_{tg} = \frac{\sigma_{\max}}{\sigma_{nom}} = \frac{\sigma_{\max}}{\sigma} = \frac{\sigma_{\max}(H-d)h}{P} = K_{tg}\frac{H-d}{H} \qquad \text{Eq. 13}$$

In general, K_{tg} and K_{tn} are different. As d/H increases from 0 to 1, K_{tg} increases from 3 to ∞, whereas K_{tn} decreases from 3 to 2. Either K_{tn} or K_{tg} can be used in calculating the maximum stress. It would appear that K_{tg} is easier to determine as σ is immediately evident from the geometry of the bar. But the value of K_{tg} is hard to read from a stress concentration plot for $d/H > 0,5$, since the curve becomes very steep. In contrast, the value of K_{tn} is easy to read, but it is necessary to calculate the net cross-sectional area to find the maximum stress. Since the stress of interest is usually on the net cross section, K_{tn} is the more generally used factor. In addition, in a fatigue analysis only K_{tn} can be used to calculate the stress gradient correctly. In conclusion, normally it is more convenient to give stress concentration factors using reference stresses based on the net area rather than the gross area.

2.4 Theoretical Stress Concentartion Factor

An import source of the library of engineering mechanics about the stress concentration factor is the work of R.E Peterson [2] who compiled them from his own work and that of others. Peterson developed the style of presentation in which the stress-concentration factor K_t is multiplied by the nominal stress σnom to estimate the magnitude of the largest stress

in the locality. His approximations were based on photo elastic studies of two-dimensional strips (Hartman and Levan 1951, Wilson and White 1973), with some limited data from three-dimensional photo elastic tests of Hartman and Levan.

Then, in order to evaluate the stress concentration factor there is the above equation:

$$K_t = C_1 + C_2(\frac{2t}{D}) + C_3(\frac{2t}{D})^2 + C_4(\frac{2t}{D})^3 \qquad \text{Eq. 14}$$

with

$$C_1 = 0,926 + 1,157\sqrt{\frac{t}{r}} - 0,099\frac{t}{r} \qquad \text{Eq. 15}$$

$$C_2 = 0,012 - 3,036\sqrt{\frac{t}{r}} + 0,961\frac{t}{r} \qquad \text{Eq. 16}$$

$$C_3 = -0,302 + 3,997\sqrt{\frac{t}{r}} - 1,744\frac{t}{r} \qquad \text{Eq. 17}$$

$$C_4 = 0,365 - 2,098\sqrt{\frac{t}{r}} + 0,878\frac{t}{r} \qquad \text{Eq. 18}$$

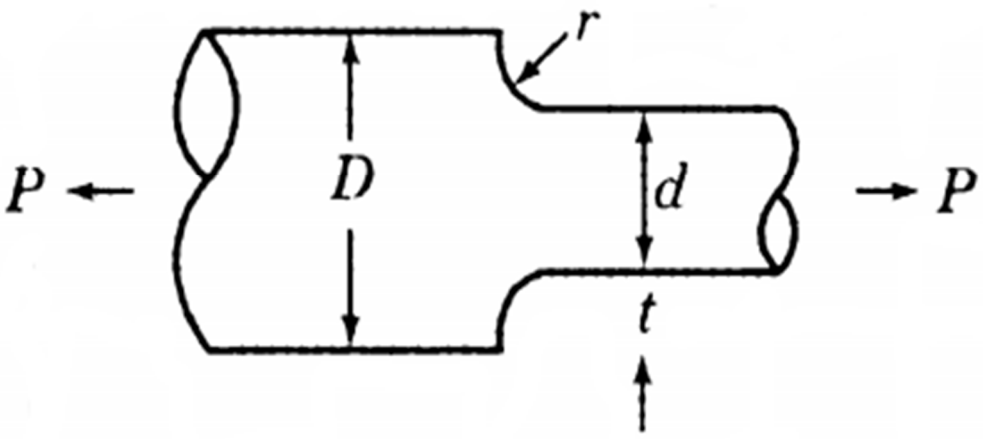

Figure 11 Shoulder fillet geometry.

Due to the geometry Figure 11 of the problem it appears that $r = \frac{D-d}{2}$ and this leads to $t/r = 1$ for all the elements. Thus, the values of C_1, C_2, C_3 and C_4 are:

$$C_1 = 1,984,\ C_2 = -2,063,\ C_3 = 1,951,\ C_4 = -0,855$$

2.5 Notch Sensitvity

The theoretical stress concentration factors apply mainly to ideal elastic materials and depend on the geometry of the body and the loading. Sometimes a more realistic model is preferable. When the applied loads reach a certain level, plastic deformations may be involved. The actual strength of structural members may be quite different from that derived using theoretical stress concentration factors, especially for the cases of impact and alternating loads. It is reasonable to introduce the concept of the effective stress concentration factor K_e .This is also referred to as the factor of stress concentration at rupture or the notch rupture strength ratio. The magnitude of K_e is obtained experimentally. For instance, K_e for a round bar with a circumferential groove subjected to a tensile load P' (Figure 12a) is obtained as follows:

1. Two sets of specimens of the actual material, the round bars of the first set having circumferential grooves, with d as the diameter at the root of the groove (Figure 12a). The round bars of the second set are of diameter d without grooves (Figure 12b).
2. In a tensile test for the two sets of specimens, the rupture load for the first set is P', while the rupture load for second set is P.
3. The effective stress concentration factor is defined as:

$$K_e = \frac{P}{P'} \qquad \text{Eq. 19}$$

In general, $P' > P$ so that $K_e > 1$.The effective stress concentration factor is a function not only of geometry but also of material properties. Some characteristics of K_e for static loading of different materials are discussed briefly below.

1. Ductile material. A tensile loaded plane element with a V-shaped notch. The material law for the material is sketched in Figure 13. If the maximum stress at the root of the notch is less than the yield strength $\sigma_{\max} < \sigma_y$ the stress distributions near the notch would appear as in curves 1 and 2 in Figure 13. The maximum stress value is:

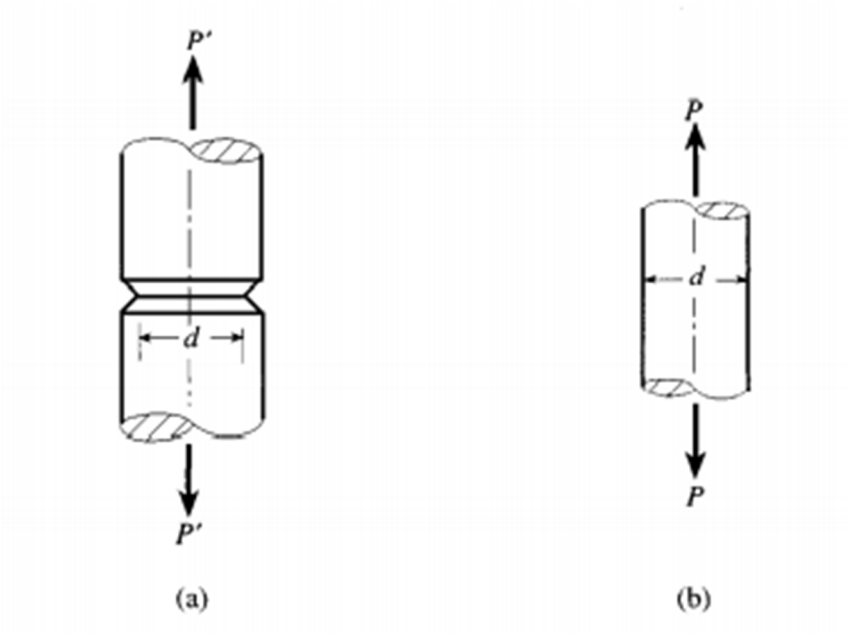

Figure 12 Specimens for obtaining K_e.[2]

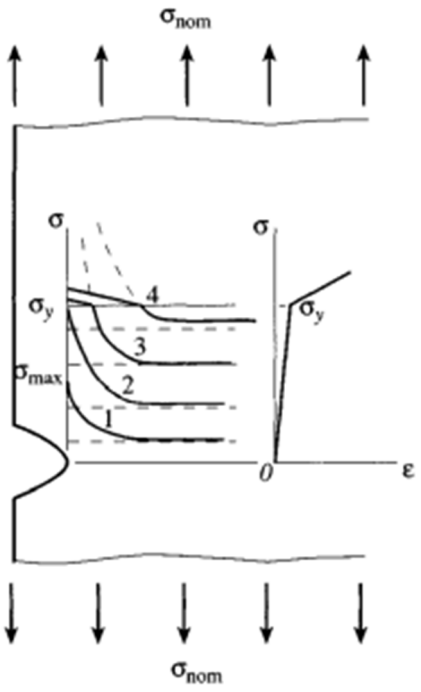

Figure 13 Stress distribution near a notch for a ductile material.[2]

$$\sigma_{\max} = K_t \sigma_{nom} \qquad \text{Eq. 20}$$

As the $\sigma_{\max}$ exceeds σ_y, the strain at the root of the notch continues to increase but the maximum stress increases only slightly. The stress distributions on the cross section will be of the form of curves 3 and 4 in Figure 13. Equation above no longer

applies to this case. As σ_{nom} continues to increase, the stress distribution at the notch becomes more uniform and the effective stress concentration factor K_e is close to unity.

2. Brittle material. Most brittle materials can be treated as elastic bodies. When the applied load increases, the stress and strain retain their linear relationship until damage occurs. The effective stress concentration factor K_e is the same as K_t.
3. Gray cast iron. Although gray cast irons belong to brittle materials, they contain flake graphite dispersed in the steel matrix and a number of small cavities, which produce much higher stress concentrations than would be expected from the geometry of the discontinuity. In such a case the use of the stress concentration factor K_t may result in significant error and K_e can be expected to approach unity, since the stress raiser has a smaller influence on the strength of the member than that of the small cavities and flake graphite.

It can be reasoned from these three cases that the effective stress concentration factor depends on the characteristics of the material and the nature of the load, as well as the geometry of the stress raiser. Also $1 \le K_e \le K_t$. The maximum stresses at rupture can be defined to be:

$$\sigma_{\max} = K_e \sigma_{nom} \qquad \text{Eq. 21}$$

To express the relationship between K_f and K_t, introduce the concept of notch sensitivity q (Boresi 1993):

$$q = \frac{K_e - 1}{K_t - 1} \qquad \text{Eq. 22}$$

Or

$$K_e = q(K_t - 1) + 1 \qquad \text{Eq. 23}$$

And the $\sigma_{\max}$ can be defined as:

$$\sigma_{\max} = \left[q(K_t - 1) + 1 \right] \sigma_{nom} \qquad \text{Eq. 24}$$

If $q = 0$, then, meaning that the stress concentration does not influence the strength of the structural member. If $q = 1$, then $K_e = K_t$ implying that the theoretical stress concentration factor should be fully invoked. The notch sensitivity is a measure of the agreement between K_e and K_t. The concepts of the effective stress concentration factor and notch sensitivity are used primarily for fatigue strength design. For fatigue loading:

$$K_f = \frac{Fatigue \text{ limit of unnotched specimen(axial or bending)}}{Fatigue \text{ limit } of \text{ notched specimen(axial or bending)}} = \frac{\sigma_f}{\sigma_{nf}} \quad \text{Eq. 25}$$

$$K_{fs} = \frac{Fatigue \text{ limit of unnotched specimen(shear stress)}}{Fatigue \text{ limit } of \text{ notched specimen(shear stress)}} = \frac{\tau_f}{\tau_{nf}} \quad \text{Eq. 26}$$

Where K_f is the fatigue notch factor for normal stress and K_{fs} is the fatigue notch factor for shear stress, such as torsion. The notch sensitivities for fatigue become:

$$q = \frac{K_f - 1}{K_t - 1} \quad \text{Eq. 27}$$

or

$$q = \frac{K_{fs} - 1}{K_{ts} - 1} \quad \text{Eq. 28}$$

The values of q vary from $q = 0$ for no notch effect ($K_f = 1$) to $q = 1$ for the full theoretical effect ($K_f = K_t$).

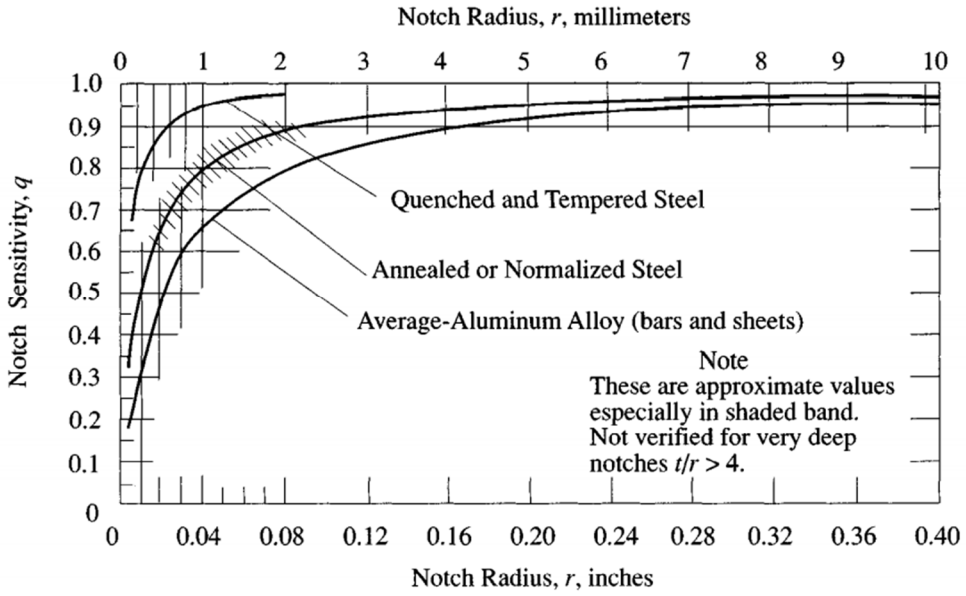

Figure 14 Average fatigue notch sensitivity[2].

Where K_{tf} is the estimated fatigue notch factor for normal stress, a calculated factor using an average q value obtained from Figure 14 or a similar curve, and K_{tsf} is the estimated fatigue notch factor for shear stress.

2.6 Influence from Poisson's Ratio

In the charts for stress concentration found in the literature it is never, to the authors knowledge, specified what value of Poisson's ratio, ν, that have been applied. Many original charts have been made from photo elastic experiments, not using steel. In (Dally & Riley 1991) it is stated that the influence from Poisson ratio on the result is usually small, meaning less than 7%. In relation to optimization this difference is not negligible since the improvement in the stress level is of the same order typically (Figure 15).

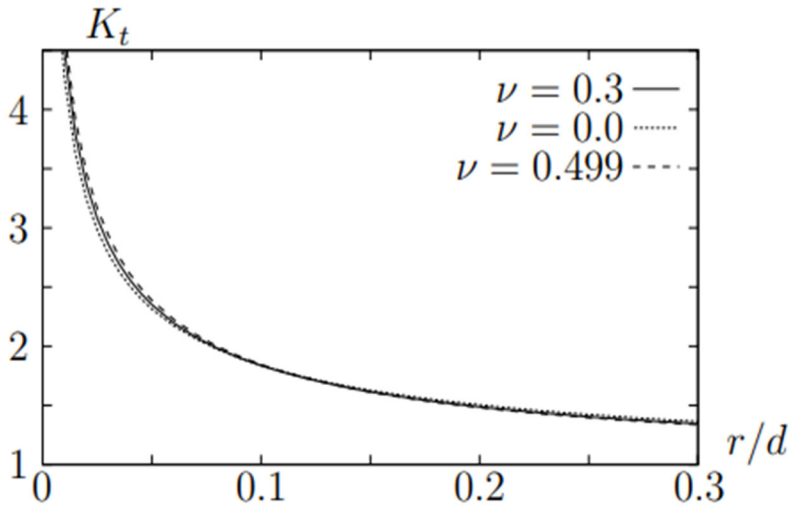

Figure 15 Influence of the Poisson's ratio on the stress concentrations factors for shaft fillet in bending [4].

To exemplify the influence from Poisson's ratio the stress concentration for bending defined as:

$$\mathrm{K}_t = \frac{\sigma_{\max}}{\sigma_{nom}} \qquad \text{Eq. 29}$$

Where $\sigma_{\max}$ is the maximum principal stress and the nominal stress is defined as:

$$\sigma_{nom} = \frac{32M_b}{\pi d^3} \qquad \text{Eq. 30}$$

For a specific value $D/d = 0,3$.

From Figure 7 it is seen that overall, the influence from v is small but not negligible especially for the low values of r/d. In the graph the highest deviation found is:

$$\frac{K_t(v = 0,499) - K_t(v = 0)}{K_t(v = 0,3)} \approx 0.1 \qquad \text{Eq. 31}$$

This is a 10% difference. For the highest value of r/d shown the deviation is approximately 2%. In the previous part of the paper when not specified and in the remaining part of the paper we will assume that $v = 0,3$ corresponding to the normal value for a steel shaft.

Chapter 3

3.1 Finite Elements Method

The most powerful tool that engineers use to solve a wide range of problems is the **Finite Elements Method** (FEM). This method covers both linear and non-linear problems (strain-displacement) of continues parts as well as problems of any kind of flow such as heat, fluids, and magnetic flow. Their modeling thanks to the developments of computers and cad systems in general is now quite easy even in complex problems. Due to this development, it is necessary to keep up with the technology and modeling techniques that are applied in various professional computer programs such as the ANSYS, NASTRAN, and ABAQUS. This method overcomes many obstacles presented by the classical approximation methods because the regions are distinguished into simple geometric shapes which are called finite elements **(**Figure 16**)**. The relationships that are used and the properties of the materials are considered on these elements and are expressed in terms of unknown values in their angles which respond in relation to the finite element and are called its nodes. A correct synthesis with correctly considered loads and correct constraints is a set of equations with the solution of which we see the behavior of a continuous body defined by a complex region. The above equations appear in the normal form of a differential equation system with respect to the temporal responses of the nodes. Since the response to every internal point of every finite element of the material is a known function of the responses of the nodes of the element, the solution of the equations leads to the determination of the complete response of the body.

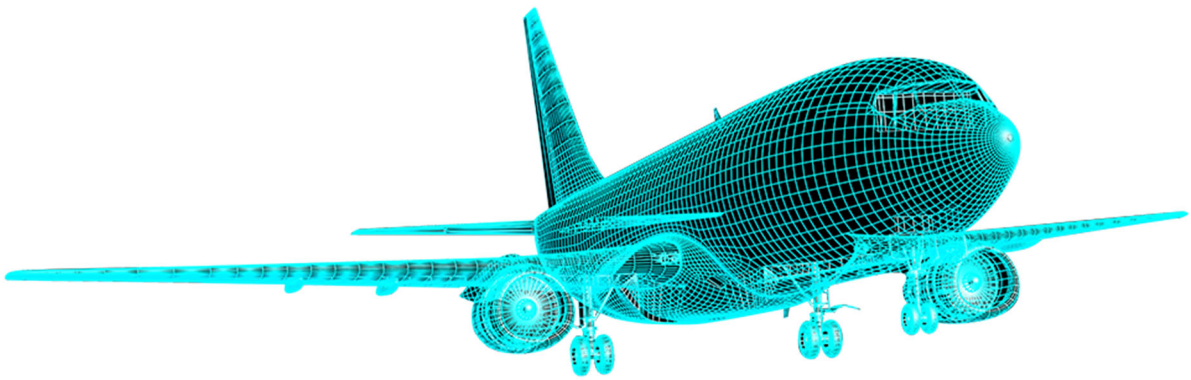

Figure 16 The fuselage of an airplane divided to finite elements.

3.2 FEM Modeling Shafts

Static strength evaluation of components (machine elements) makes the modeling and estimation of stress concentrations the important point. This evaluation demands a high number of FEM meshing nodes on the boundary shape where the stress concentration is present. For a given design, the standard circular fillet shapes the position of high stress can be found and the element refinement can be done locally at this specific point reducing the need for overall mesh refinement considerably. In optimization where we seek to lower the maximum stress the point of maximum stress is not known but is a function of the design. In fact, the optimality criterion for minimum stress on the surface is that the stress is constant on the surface, which will increase the number of nodes on the boundary since we need to evaluate the stress over a larger area.

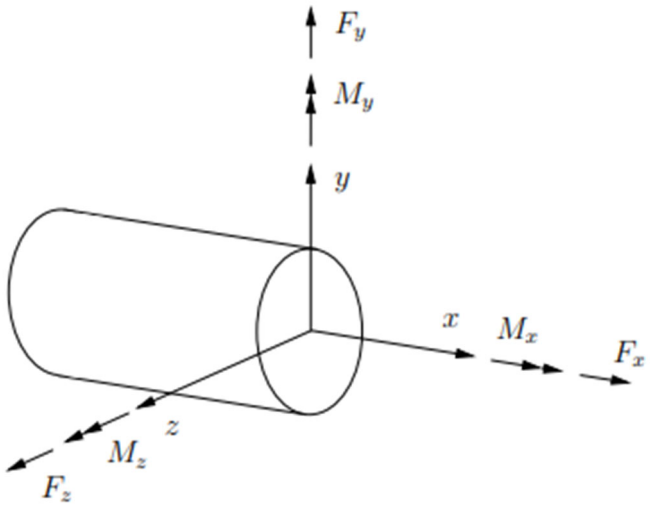

Figure 17 Definitions of forces and moments on a beam cross section [5]

In Figure 17 the possible forces and moments on a shaft are shown, axial load F_x , torsional load M_x . The bending moment is $M_b = \sqrt{M_y{}^2 + M_z{}^2}$. The total shear force $F_s = \sqrt{F_z{}^2 + F_y{}^2}$ is normally not accounted for because the shear stress associated with this force is zero at the point of maximum normal stress due to the bending moment. The shaft geometry is axisymmetric and only the axial load is also axisymmetric. FEM modeling of the shaft can be done in many ways. For the axial load the simplest modeling is to use a standard axisymmetric model. For torsional load, the loading is out-of-plane relative to the plane of a 2D axisymmetric model, and this cannot be done with standard axisymmetric modeling. A full 3D shaft

modeling can of course be used but due to the symmetry we can reduce the 3D model to a sector of a circle where the central angle in principle can go to zero, but this will be limited by the resulting FEM mesh quality.[5]

3.3 Diploma Thesis

The most common problem in any mechanical construction is the determination of the stress load that develops as well as the critical values that causes the failure. Almost any mechanical structure consists of shafts that receive the most stress. These shafts in order to accommodate some mechanical elements such as (gears, pulleys, and flywheels) are designed with geometrical discontinuities. The type of discontinuity that is most common appear in these circumstances is the shoulder fillet. In this geometry the diameter D of a shaft decreases to a smaller diameter d under a shoulder fillet process with r radius.

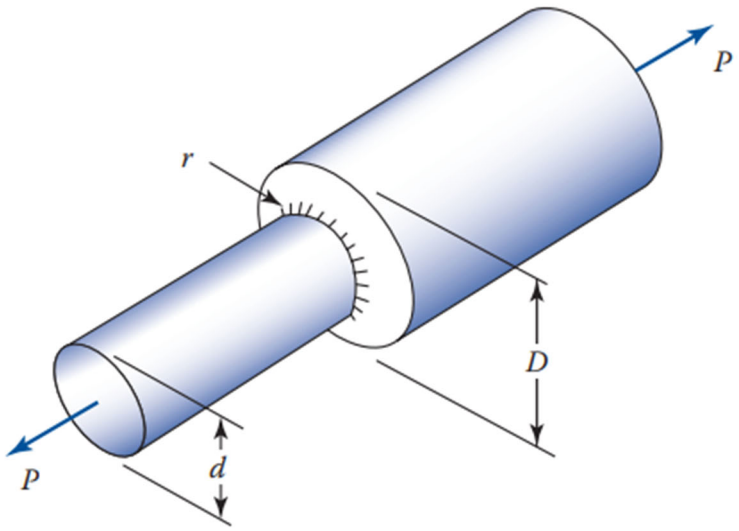

Figure 18 Diploma thesis shaft.

In the science of mechanics, this change of geometry causes stress concentrations in discontinuous regions. The unique parameter that allows us to determine the stress load in this situation is the stress concentration factor (Kt, SCF). The stress concentration factor values are affected only by the geometry of the specimen and specifically by the r/d. This project targets to calculate the stress concentration factor by the method of finite elements and to compare them with the theoretical results. For this experiment, the shaft is under axial load

of tension and the procedure will be applied for five different geometries with the same length $L = 180mm$ (Table 2).

Specimen	$D(mm)$	$d(mm)$	$r(mm)$	D/d	r/d
3010	40	36	1,8	1,11	0,05
3075	40	34,7826	2,6087	1,15	0,075
3015	40	30,7692	4,6154	1,3	0,15
3025	40	26,6666	6,6667	1,5	0,25
3030	40	25	7,5	1,6	0,3

Table 2 Geometry of the examined specimens

3.4 Abacus 2D Axisymmetric Problem.

This project is analyzed on abaqus environment. The investigated stress concentration cases are considered as axisymmetric problem for a shoulder fillet shaft subjected to axial tension. For this kind of geometry, it can be used cylindrical coordinates (Figure 19). Then, in any cylindrical problem the solution is going to be independent of the angle Θ. Thus, the problem could be considered as a two-dimensional problem and axisymmetric elements could be used.

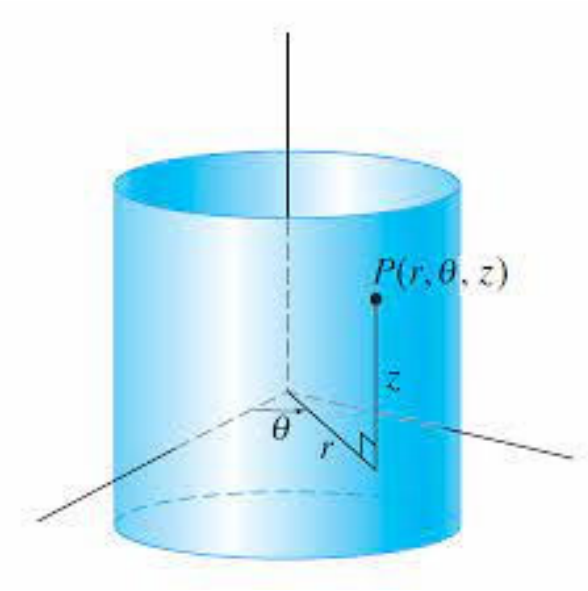

Figure 19 Cylindrical coordinates on a cylindrical element.

For this purpose, the first step is to create a part in abaqus environment of the half geometry where the loads and the border conditions will be applied (Figure 20). In the specimen a tensile stress is applied to one end while the other end is anchored.

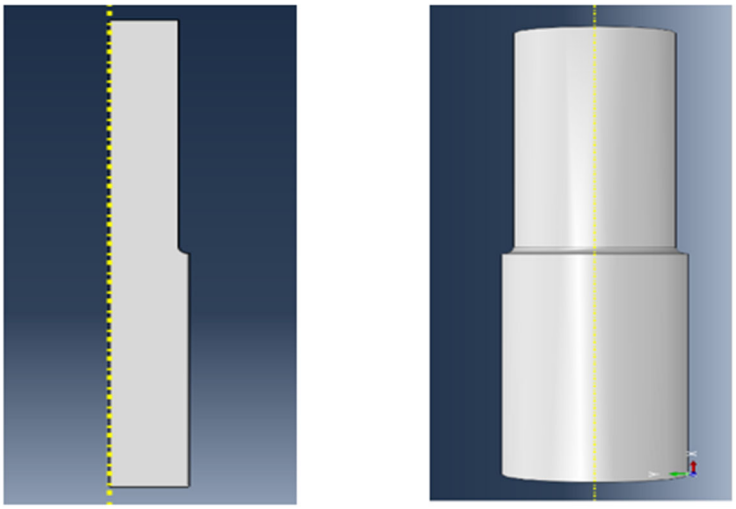

Figure 20 Axisymmetric part and 3-D part.

3.5 Abaqus Modeling Axisymetric Problem

3.5.1 Border Conditions

The simulation of boundary conditions and other forms of constraint is probably the single most difficult part of the accurate modeling of a structure for a finite element analysis. In specifying constraints, it is relatively easy to make mistakes of omission or misrepresentation. It may be necessary for the analyst to test different approaches to model esoteric constraints such as bolted joints, welds, which are not as simple as the idealized pinned or fixed joints. Testing should be confined to simple problems and not to a large, complex structure. Sometimes, when the exact nature of a boundary condition is uncertain, only limits of behavior may be possible. For example, we have modeled shafts with bearings as being simply supported. It is more likely that the support is something between simply supported and fixed, and we could analyze both constraints to establish the limits. However, by assuming simply supported, the results of the solution are conservative for stress and deflections. That is, the solution would predict stresses and deflections larger than the actual. Multipoint constraint equations are quite often used to model boundary conditions or rigid connections between

elastic members. When used in the latter form, the equations are acting as elements and are thus referred to as rigid elements. Rigid elements can rotate or translate only rigidly. Boundary elements are used to force specific nonzero displacements on a structure.

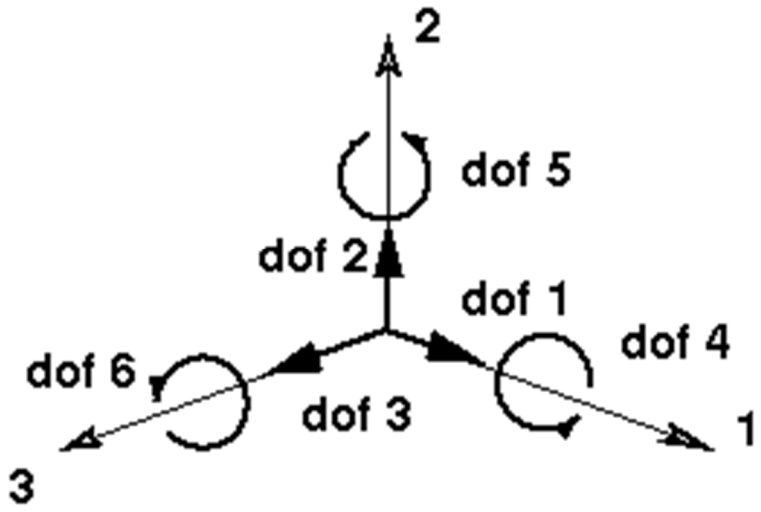

Figure 21 Displacements on the three directions.

1. Translation in the 1-direction(U1)
2. Translation in the 2-direction (U2)
3. Translation in the 3-direction (U3)
4. Rotation about the 1-direction (UR1)
5. Rotation about the 2-direction (UR2)
6. Rotation about the 3-direction (UR3)

The first border condition is applied at the axis of symmetry in the 1 direction. (Figure 22)

- $U_1 = 0$ Eq. 32
- The second border condition is applied on the bottom of the specimen which is anchored (Figure 22).
- $U_1 = 0$ Eq. 33
- $U_2 = 0$ Eq. 34

3.5.2 Tensile Load

There are two basic forms of specifying loads on a structure-nodal and element loading. However, element loads are eventually applied to the nodes by using equivalent nodal loads. One aspect of load application is related to Saint-Venant's principle. If one is not concerned about the stresses near points of load application, it is not necessary to attempt to distribute the loading very precisely. The net force and moment can be applied to a single node, provided the element supports the do associated with the force and moment at the node. However, the analyst should not be surprised, or concerned, when reviewing the results and the stresses in the vicinity of the load application point are found to be very large. Concentrated moments can be applied to the nodes of beam and most plate elements. However, concentrated moments cannot be applied to truss, two-dimensional plane elastic, axisymmetric, or brick elements. For the situation of an axisymmetric problem under tension, the tensile stress is applied at the top of each specimen and has the value of 350 MPa**.** (Figure 22)

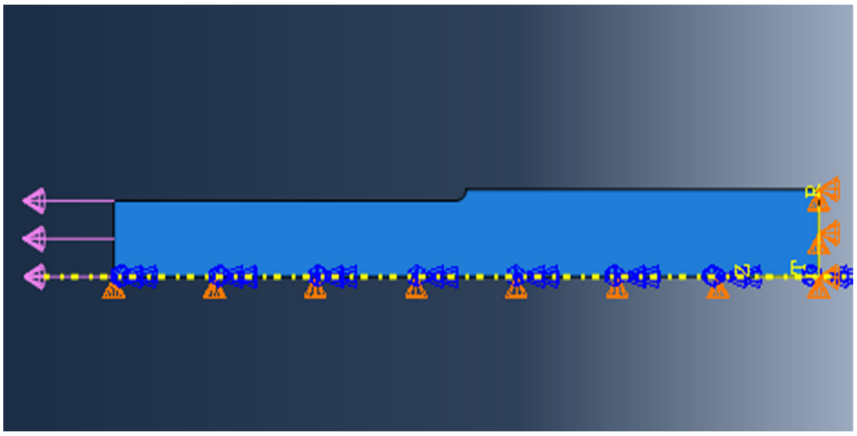

Figure 22 Border conditions and tensile load.

3.5.3 Partitions and Mesh

The network of elements and nodes that discretize a region is referred to as a mesh. The mesh density increases as more elements are placed within a given region. Results generally improve when the mesh density is increased in areas of high stress gradients and when geometric transition zones are meshed smoothly. Generally, but not always, the FEA results converge toward the exact results as the mesh is continuously refined. There are three basic

ways to generate an element mesh, manually, semi automatically, or fully automatically. For this project it is necessary to create a mesh with different shape of elements in order to evaluate better the stress allocation around the discontinuity. After many attempts, the mesh construction became a manually procedure. The right size of the elements in the notch should be one twentieth of the radius (r) of curvature. However, as the elements are removed from the notch they should be increased in size. If the density of the grid were the same throughout the length of the specimen, it would have the effect of increasing the number of degrees of freedom of the problem and consequently the time of its solution by the computer without any different result. Thus, more interest is given to the accuracy of the stress value at the depth of the notch, where the phenomenon of stress concentration occurs and not in remote areas of the specimen where the phenomenon is less intense. In the finite element method, the higher the number of elements and therefore the number of degrees of freedom the more the accuracy of the results increases. The structure of the mesh that is applied at the shafts is designed according previous study [3].

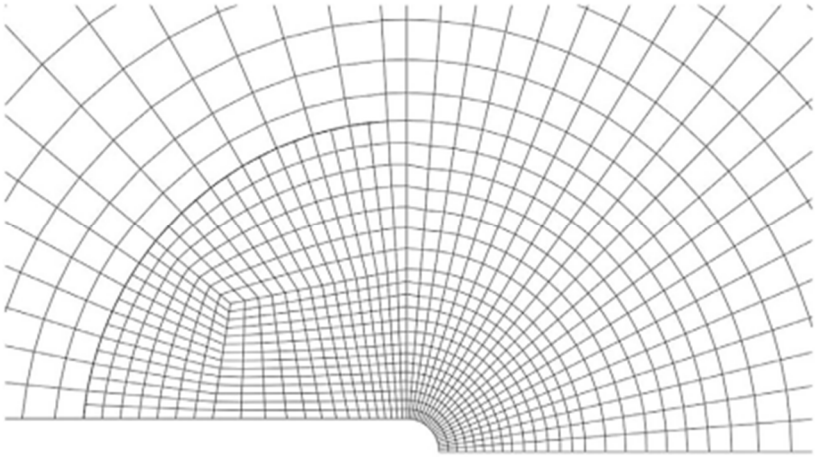

Figure 23 Finite element mesh in the crack-tip region [3]

To accomplish this type of mesh it is necessary to create the right partitions for each specimen. The creation of the partitions and the final mesh of the first geometry of the 3075 specimen are obtained in the Figure 24 and Figure 25.

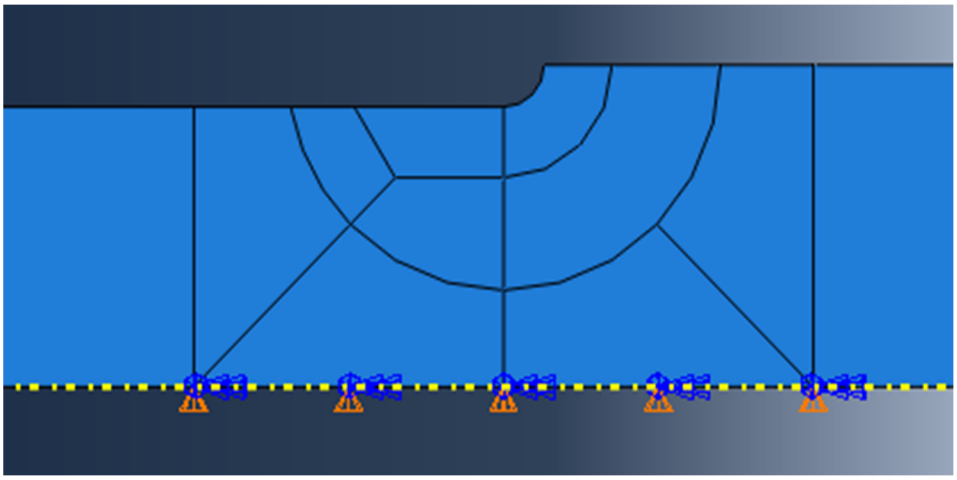

Figure 24 Partition of 3075 specimen.

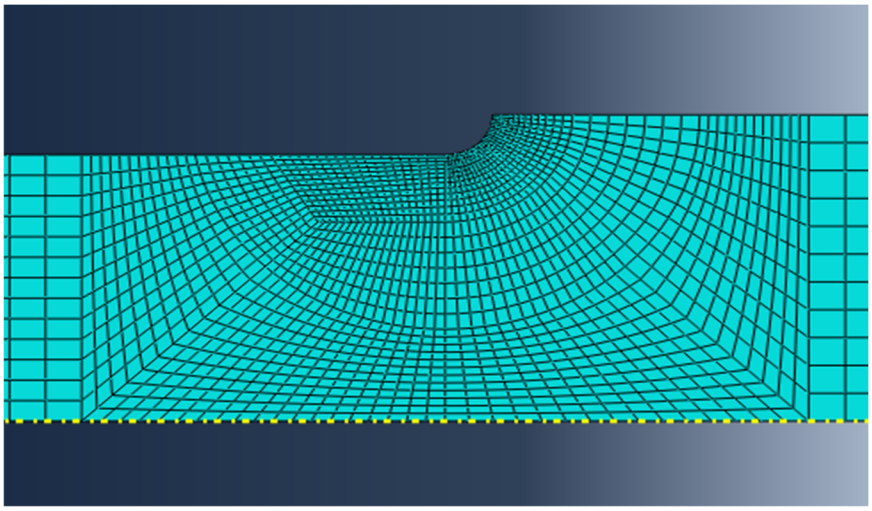

Figure 25 Mesh in 3075 specimen.

At this point it should be mentioned that there was a need to design a different grid for each essay. It was not possible to use one grid for all specimens. This is due to the fact that each specimen had a different radius of curvature resulting in an increase or decrease in the density of the grid in that area giving wrong results. Finally, the grids used for each test are different but have the same total number of elements (2946) and in the area near the notch they have the same density.

3.6 CAX4R Elements

There are many different categories of elements to create a mesh construction in abaqus. The type of element that it is appropriate for each circumstance are defined by the geometry of the specimen and the loads that are applied. In order to appreciate the advantages and limitations of each element type, it is important to understand both the nomenclature and underlying fundamentals governing finite element behavior in Abaqus. Towards that goal, there are five aspects of an element that characterize its behavior in Abaqus:

- Family
- Degrees of Freedom
- Number of Nodes
- Formulation
- Integration

The element family, Figure 26, is used to describe the type of element and hint at applications for which it may be suitable. The major distinction between element families is the geometry type that each family assumes.

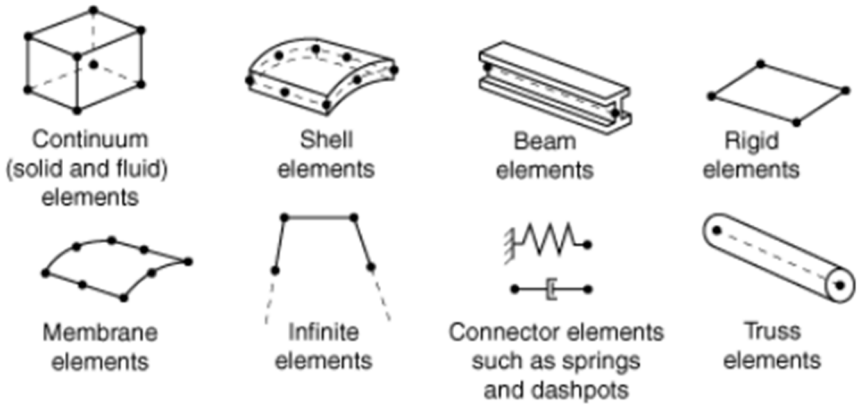

Figure 26 Commonly used element families [6]

Abaqus has several classes of two-dimensional continuum elements that differ from each other in their out-of-plane behavior. Two-dimensional elements can be quadrilateral (CPE4R, CPS4R, and CAX4R) or triangular (CPE3, CPE6M, CPS3, CPS6M, CAX3, and CAX6M) (Figure 27).

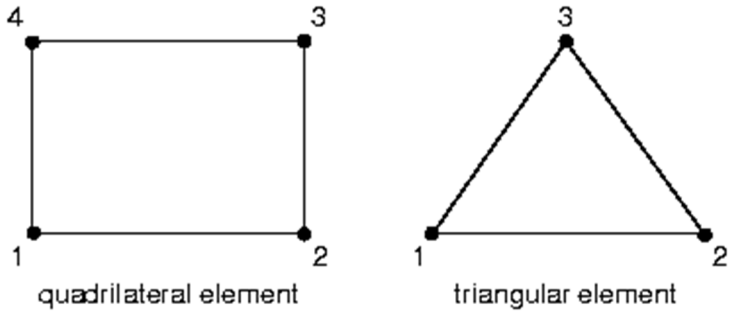

Figure 27 Two-dimensional elements [6]

The CAX4R elements are the suitable tool to model an axisymmetric problem in Abaqus environment. The (r) and the (z) directions coincide with the global X and Y axis respectively. The structured is supposed to be symmetric about the (z) axis. The point loads are defined as the total loads integrated around the circumference and the distributed loads should be provided as loads per unit surface area (Figure 28).

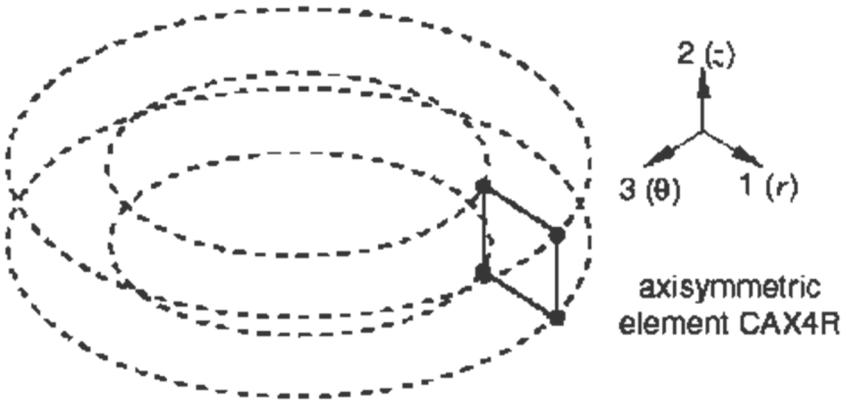

Figure 28 Axisymmetric elements. [6]

3.7 Final Mesh and Stress Distribution.

The following figures show the stress distribution for the specimens as calculated after processing the data in the ABAQUS environment. It is obvious that the maximum values of tension are actually displayed at the depth of the notch symmetrically of the specimen. To evaluate the entire specimen, it is just needed to rotate the 2-D specimen to 360 degrees and the problem has the same results with a 3-D analysis (Figure 34).

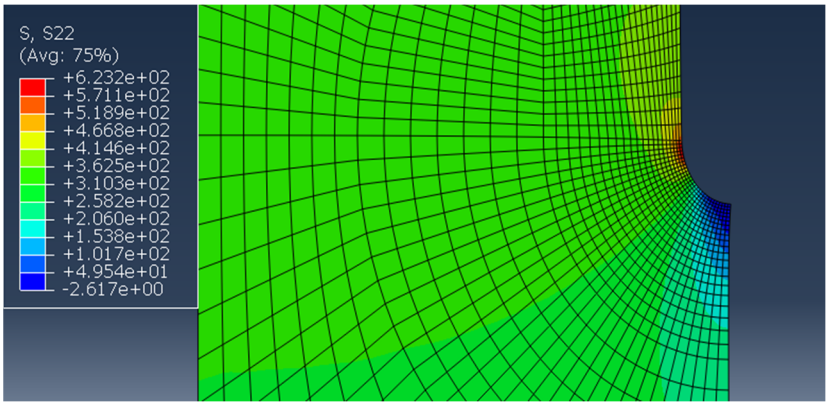

Figure 29 Stress distribution across the 3010 element in abaqus environment.

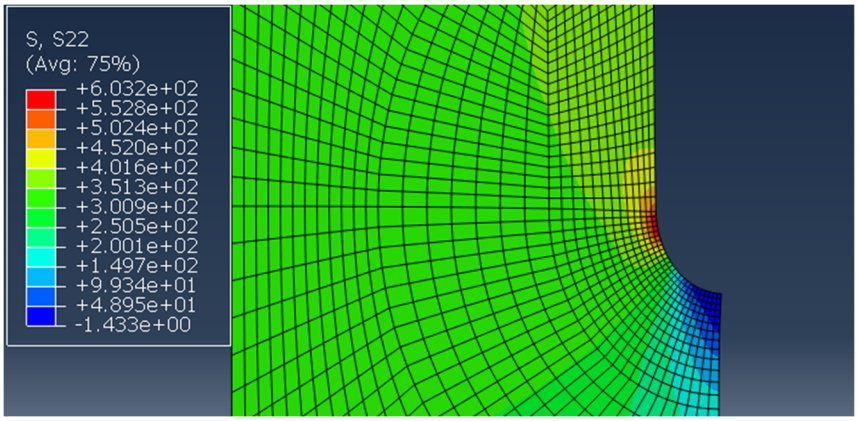

Figure 30 Stress distribution across the 3075 element in abaqus environment.

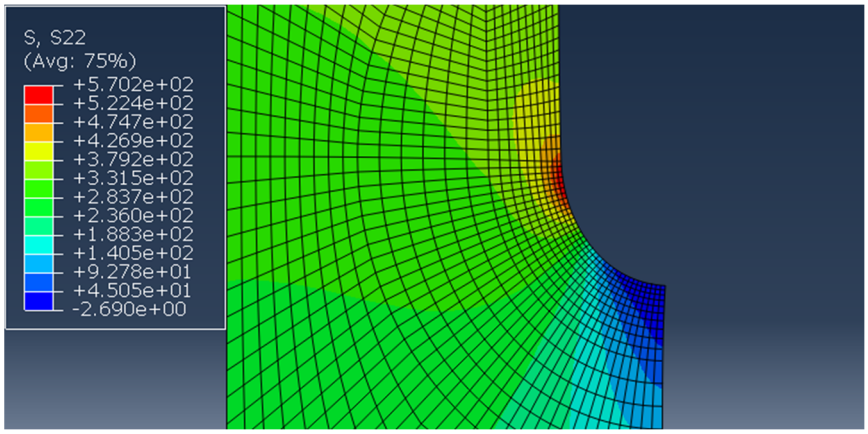

Figure 31 Stress distribution across the 3015 element in abaqus environment.

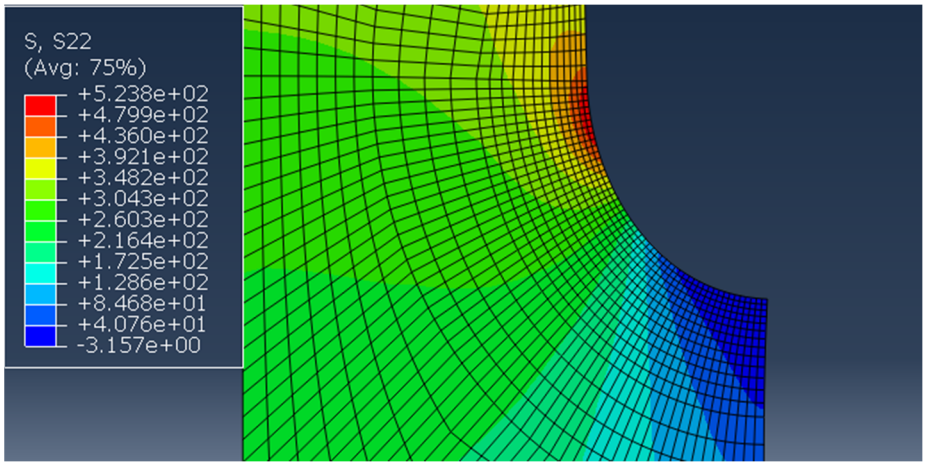

Figure 32 Stress distribution across the 3025 element in abaqus environment.

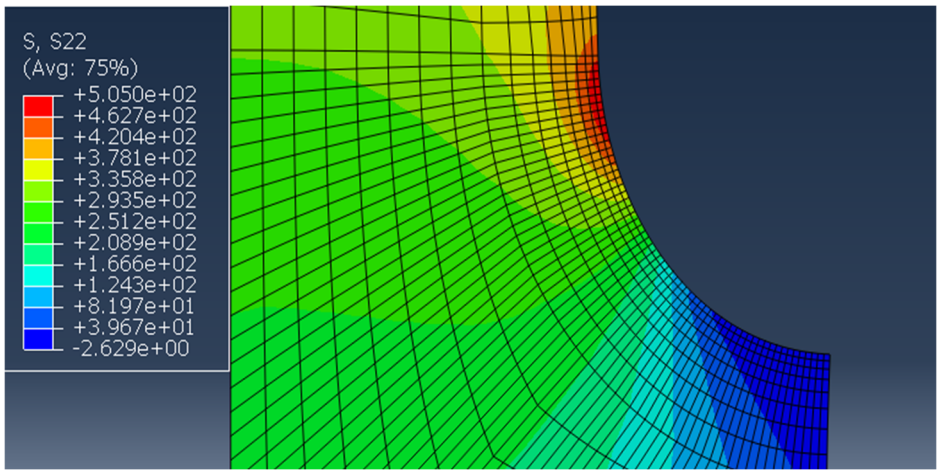

Figure 33 Stress distribution across the 3030 element in abaqus environment.

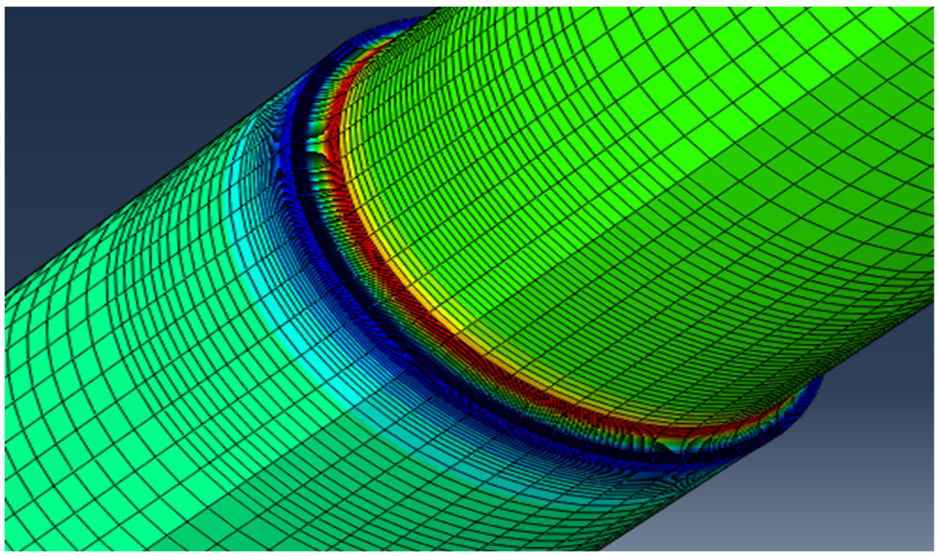

Figure 34 Stress distribution across the 3-D element in abaqus environment.

Chapter 4

4.1 FEM Analysis Results

After designing the specimens, the grid, the appropriate boundary conditions the specimens are loaded. The material of the specimen does not need to be stated as the problem is solved dimensionless. All that needs to be stated is the module of elasticity E, which is approximately the same for all steels ($210GPa$). For the five different specimens the results are given accurately in the table below. In the same table are listed for comparison the values of the stress concentration factor as they appear from the Pilkey and Peterson diagrams (Table 3).

Specimen	$\sigma_{nominal}(MPa)$	$\sigma_{22}FEM(MPa)$	K_t Peterson	K_t FEM	$Error\%$
3010	350	623,35	1,81335	1,781	1,7838
3075	350	603,2	1,74587	1,72343	1,28529
3015	350	570,199	1,60025	1,62914	1,80559
3025	350	523,79	1,47922	1,49657	1,17301
3030	350	505	1,43683	1,44286	0,4192

Table 3 Abaqus results and stress comparison for different geometries.

The following figure (Figure 35) shows the stress consumption for the 3075 specimen, it is similar to the other specimens, in a section made at the beginning of the notch. The red curve shows the stress distribution when the specimen is not notched and has a diameter $D = 26,666mm$ and the blue one when the specimen is notched with a shoulder fillet and an inner diameter $d = 26,666mm$ and an outer diameter $D = 40mm$.

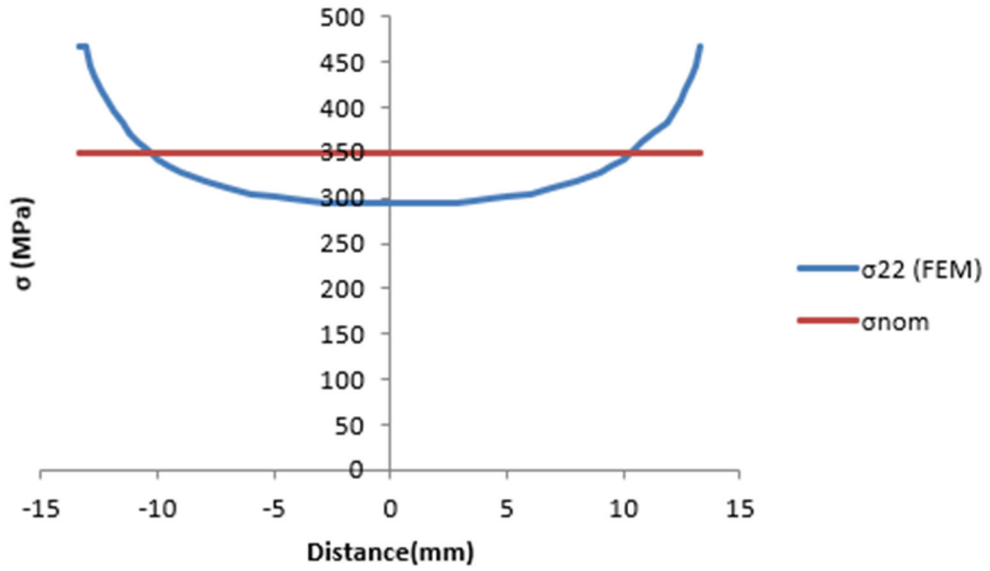

Figure 35 Stress distribution along cross section with minimum diameter d

The unnotched shaft does not appear any kind of stress concentration in all over its diameter. Although, the shoulder fillet shaft appears 43% stress increase in the outer face.

4.2 Theoretical Calculation of Stress Concentration Factor (K_t).

The exact calculation of K_t with theoretical values is appropriate in order to compare it with the Abaqus results. For this reason, the calculations are supported to the Peterson's Figure 38 and Shigley's results Figure 36.

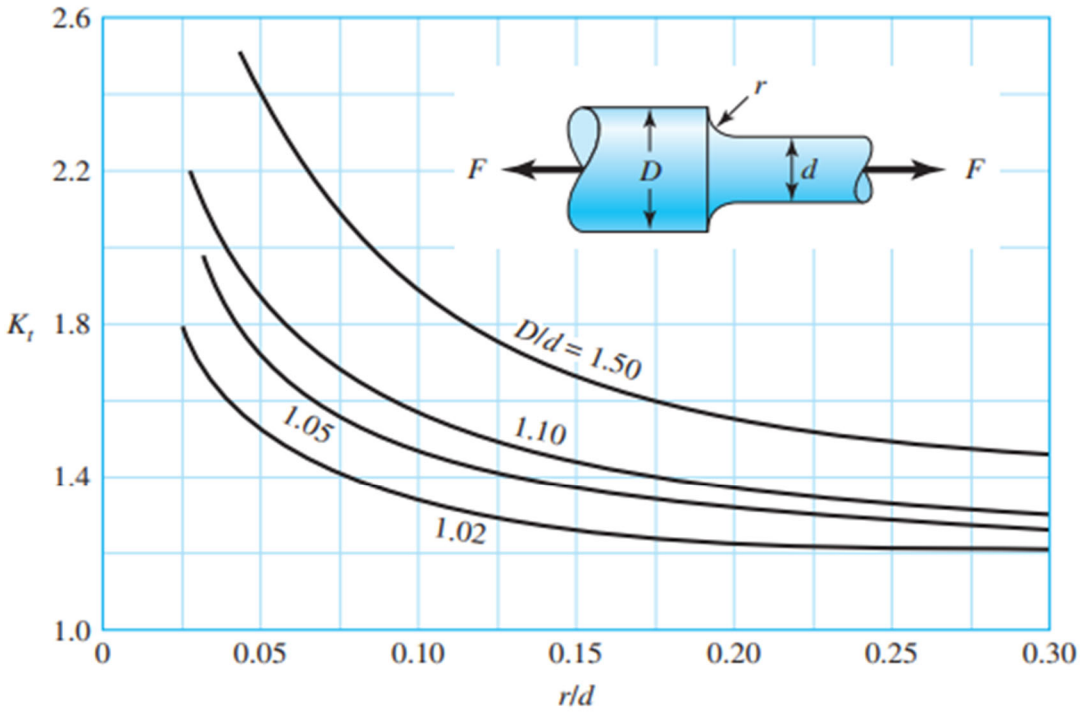

Figure 36 Shigley's chart results for Kt on shoulder fillet geometry [1]

4.3 Graphic Comparison of Kt

In the next figure there is the graphical comparison between the stress concentration factor that is calculated by the theoretical equation of Peterson and the results of the finite elements method. (Figure 37)

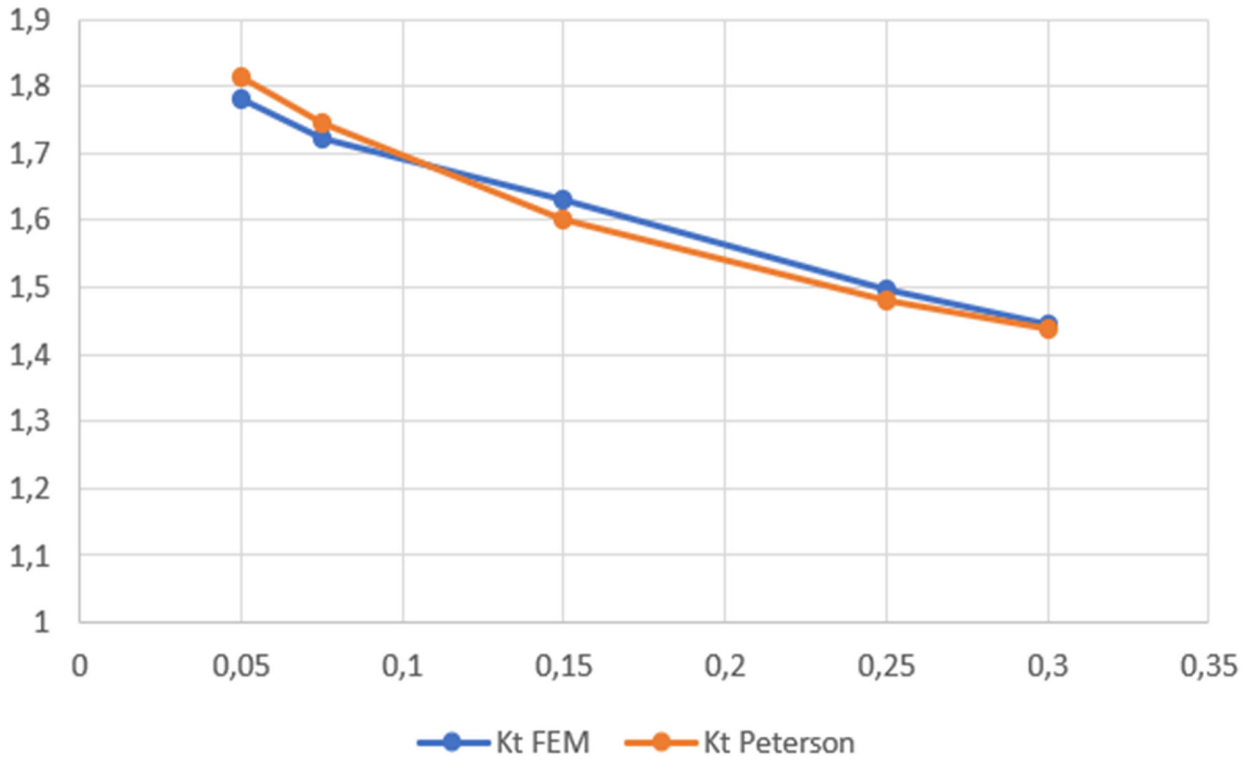

Figure 37 Graphic comparison of K_t values.

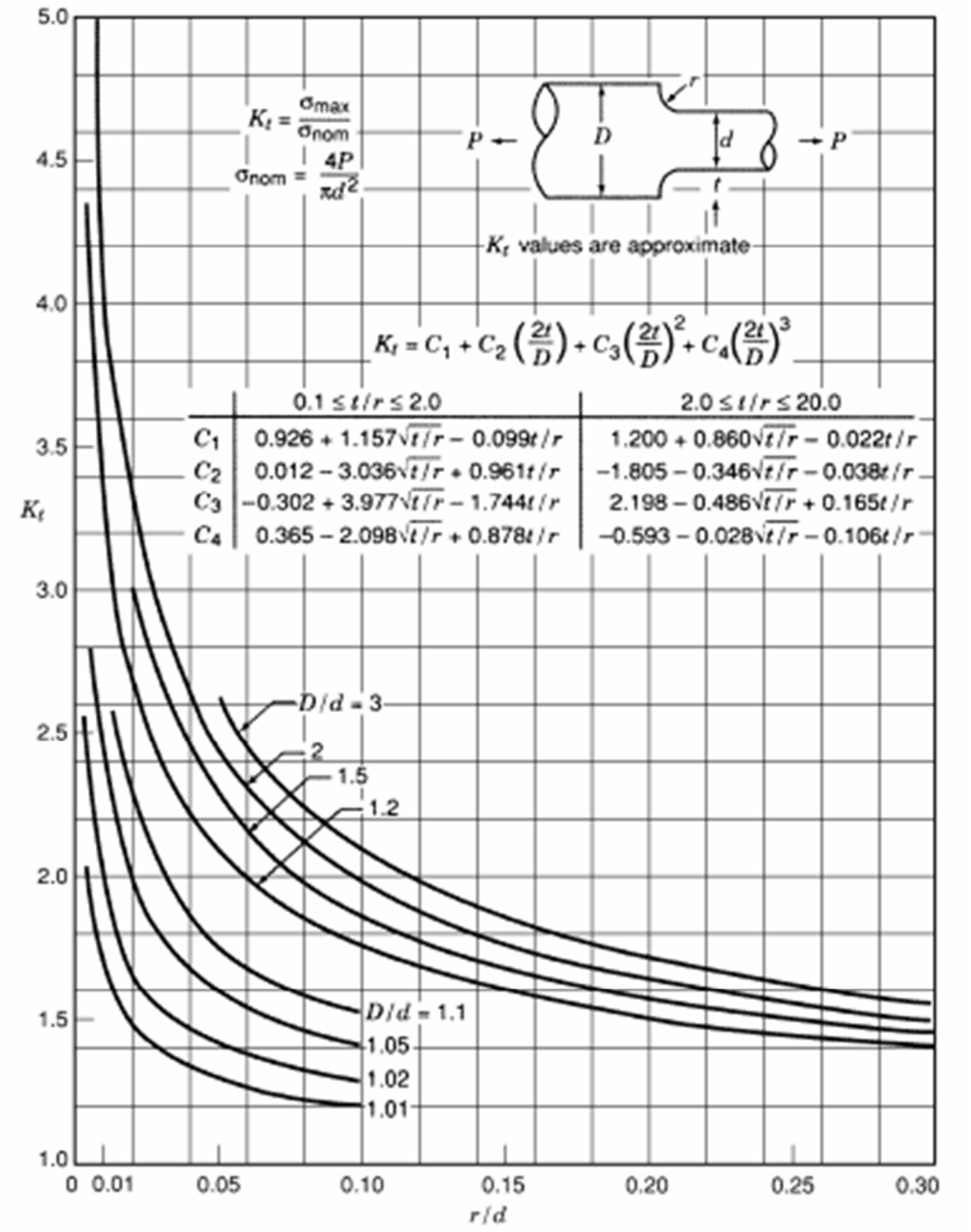

Figure 38 Peterson's stress concentration factor K_t on shoulder fillet geometry.[2]

4.4 Comments on Results

The stress concentration factor (K_t) is a crucial subject for the mechanic engineering industry and should be calculated with great accuracy. In many situations, the shape of a mechanical structure presents various geometrical discontinuities, which affect the safe function and causes failures. The Finite Element Method is a useful tool that gives the opportunity of analysis complicated geometries by the discretization technique. As mechanical engineers, our job is to anticipate structural failures and design safe models. In this project, it is presented one of the methods by which we can calculate safely and quickly the stress concentration factor (K_t). The effectiveness of this effort will be proved from the price comparison of these values with the existing ones in the literature. When the finite elements methods are applied with great accuracy the results should generally be identified with the theoretical values. In this project, as it is presented in Figure 37 and Table 3 the deviation among the results do not exceed the error of $1,8\%$. This low deviations implies, that the Finite Element Method is a accuracy way to extract a safe approach for the stress concentration factor. However, both the theoretical and the computational methods of calculating the stress concentration factor are not entirely accurate. This is due to the fact that, both methods are based on assumptions which are rarely meet in practice, such as that the material is homogeneous and isotropic. So, the mechanics should evaluate in deeper dimensions the characteristics of these problems in order to overcome any doubtful cases. In the present time, the stress concentration analysis is improving and in future time the results will help the mechanic engineers to make more steady steps to stress concentration analysis.

REFERENCES

[1] Richard G. Budynas, J. Keith Nisbett, SHIGLEY'S MECHANICAL ENGINEERING DESIGN, TENTH EDITION.

[2] Walter D. Pilkey, (1997) PETERSON'S STRESS CONCENTRATION FACTORS.

[3] N. Aravas and I. Papadioti, Journal of the Mechanics and Physics of Solids 146 (2021) 104190

[4] Dally, J. & Riley, W. (1991), Experimental stress analysis, McGraw-Hill.

[5] Pedersen, Niels Leergaard, Aspects of stress in optimal shaft shoulder fillet.

[6] https://abaqus-docs.mit.edu/2017/English/SIMACAEELMRefMap/simaelm-c-general.htm

[7] Ν. Αράβας , (2008), Μηχανική των Υλικών – Ανάλυση Ελαστικών Δοκών (τόμος ΙΙ), Πανεπιστημιακές Εκδόσεις Θεσσαλίας

APPENDIX

The input files from 3075 specimen created by abaqus environment.

```
*Heading
** Job name: Job-1 Model name: Model-1
** Generated by: Abaqus/CAE 2016.HF2
*Preprint, echo=NO, model=NO, history=NO, contact=NO
**
** PARTS
**
*Part, name=Part-1
*Node
      1,           0.,         125.
      2,          20.,         125.
      3,          20.,         180.
      4,           0.,         180.
      5,          12.,     104.7826
      6,          12.,         104.
      7,          20.,     112.7826
      8,   17.3913002,     104.7826
      9,          20.,   107.391296
     10,           0.,          55.
     11,          12.,          76.
     12,          12.,   75.2173996
     13,   17.3913002,   75.2173996
     14,          20.,   67.2173996
     15,          20.,   72.6087036
     16,          20.,          55.
     17,           0.,           0.
     18,          20.,           0.
     19,  0.909090936,         125.
     20,   1.81818187,         125.
3080,   19.3502846,   65.1998062
3081,    11.075758,   73.5326157
3082,   11.1720209,   72.9845963
3083,   11.3091803,   72.4396439
3084,   11.4868927,    71.900795
3085,    11.704587,   71.3710785
3086,   11.9614716,    70.853447
3087,   12.2565317,   70.3507996
3088,    12.588541,   69.8659515
3089,   12.9560671,   69.4016037
3090,   13.3574781,   68.9603577
3091,   13.7909527,   68.5446854
3092,   14.2544909,   68.1569061
3093,    14.745923,   67.7991867
3094,   15.2629261,   67.4735336
3095,     15.80303,   67.1817627
3096,   16.3636398,   66.9255142
3097,   16.9420452,   66.7062073
3098,   17.5354309,   66.5250854
3099,   18.1409073,   66.3831482
3100,   18.7555084,    66.281189
3101,   19.3762226,   66.2197876
```

```
*Element, type=CAX4R
  1,    1,   19,  464,  114
  2,   19,   20,  465,  464
  3,   20,   21,  466,  465
  4,   21,   22,  467,  466
  5,   22,   23,  468,  467
  6,   23,   24,  469,  468
  7,   24,   25,  470,  469
  8,   25,   26,  471,  470
  9,   26,   27,  472,  471
 10,   27,   28,  473,  472
 11,   28,   29,  474,  473
 12,   29,   30,  475,  474
 13,   30,   31,  476,  475
 14,   31,   32,  477,  476
 15,   32,   33,  478,  477
 16,   33,   34,  479,  478
 17,   34,   35,  480,  479
 18,   35,   36,  481,  480
 19,   36,   37,  482,  481
 20,   37,   38,  483,  482
 21,   38,   39,  484,  483
 22,   39,    2,   40,  484
 23,  114,  464,  485,  113
 24,  464,  465,  486,  485
 25,  465,  466,  487,  486
 26,  466,  467,  488,  487
 27,  467,  468,  489,  488
 28,  468,  469,  490,  489
```

```
2918, 3074, 3075, 3096, 3095
2919, 3075, 3076, 3097, 3096
2920, 3076, 3077, 3098, 3097
2921, 3077, 3078, 3099, 3098
2922, 3078, 3079, 3100, 3099
2923, 3079, 3080, 3101, 3100
2924, 3080,  462,  463, 3101
2925,  242, 3081,   12,   11
2926, 3081, 3082,  309,   12
2927, 3082, 3083,  310,  309
2928, 3083, 3084,  311,  310
2929, 3084, 3085,  312,  311
2930, 3085, 3086,  313,  312
2931, 3086, 3087,  314,  313
2932, 3087, 3088,  315,  314
2933, 3088, 3089,  316,  315
2934, 3089, 3090,  317,  316
2935, 3090, 3091,  318,  317
2936, 3091, 3092,  319,  318
2937, 3092, 3093,  320,  319
2938, 3093, 3094,  321,  320
2939, 3094, 3095,  322,  321
2940, 3095, 3096,  323,  322
2941, 3096, 3097,  324,  323
2942, 3097, 3098,  325,  324
2943, 3098, 3099,  326,  325
2944, 3099, 3100,  327,  326
2945, 3100, 3101,  328,  327
2946, 3101,  463,   14,  328
```

The presentation of nodes and elements is concentrated in order to diminise the size of the text. The nodes have a range between (1-3101) and the elements (CAX4R) used a range between (1-2946).

```
*Nset, nset=Set-1, generate
    1,  3101,     1
*Elset, elset=Set-1, generate
    1,  2946,     1
** Section: Section-1
*Solid Section, elset=Set-1, material=Material-1
,
*End Part
**
**
** ASSEMBLY
**
*Assembly, name=Assembly
**
*Instance, name=Part-1-1, part=Part-1
*End Instance
**
*Nset, nset=Set-1, instance=Part-1-1
   1,   4,  10,  17,  88,  89,  90,  91,  92,  93,  94,  95,  96,  97,  98,  99
 100, 101, 102, 103, 104, 105, 106, 107, 108, 109, 110, 111, 112, 113, 114, 197
 198, 199, 200, 201, 202, 203, 204, 205, 206, 207, 208, 209, 210, 211, 212, 213
 214, 215, 216, 217, 218, 219, 220, 221, 222, 223, 224, 225, 226, 227, 228, 229
 230, 231, 380, 381, 382, 383, 384, 385, 386, 387, 388, 389, 390, 391, 392, 393
 394, 395, 396, 397, 398, 399, 400, 401, 402, 403, 404, 405
*Elset, elset=Set-1, instance=Part-1-1
```

```
    1,   23,   45,   67,   89,  111,  133,  155,  177,  199,  221,  243,  265,  287,  309,  331
  353,  375,  397,  419,  441,  463,  485,  507,  529,  551,  573,  595, 1112, 1113, 1114, 1115
 1116, 1117, 1118, 1119, 1120, 1121, 1122, 1123, 1124, 1125, 1126, 1127, 1128, 1129, 1130, 1131
 1132, 1133, 1134, 1135, 1136, 1137, 1138, 1139, 1140, 1141, 1142, 1143, 1503, 1511, 1519, 1527
 2110, 2132, 2154, 2176, 2198, 2220, 2242, 2264, 2286, 2308, 2330, 2352, 2374, 2396, 2418, 2440
 2462, 2484, 2506, 2528, 2550, 2572, 2594, 2616, 2638, 2660, 2682
*Nset, nset=Set-2, instance=Part-1-1
  17,  18, 406, 407, 408, 409, 410, 411, 412, 413, 414, 415, 416, 417, 418, 419
 420, 421, 422, 423, 424, 425, 426
*Elset, elset=Set-2, instance=Part-1-1, generate
 2661,  2682,     1
*Elset, elset=_Surf-1_S3, internal, instance=Part-1-1, generate
 595,  616,    1
*Surface, type=ELEMENT, name=Surf-1
_Surf-1_S3, S3
*End Assembly
**
** MATERIALS
**
*Material, name=Material-1
*Elastic
210000., 0.3
** ----------------------------------------------------------------
**
** STEP: Step-1
**
*Step, name=Step-1, nlgeom=NO
*Static
1., 1., 1e-05, 1.
**
** BOUNDARY CONDITIONS
**


** Name: BC-1 Type: Symmetry/Antisymmetry/Encastre
*Boundary
Set-1, ZSYMM
** Name: BC-2 Type: Displacement/Rotation
*Boundary
Set-2, 1, 1
Set-2, 2, 2
**
** LOADS
**
** Name: Load-1   Type: Pressure
*Dsload
Surf-1, P, -350.
**
** OUTPUT REQUESTS
**
*Restart, write, frequency=0
**
** FIELD OUTPUT: F-Output-1
**
*Output, field, variable=PRESELECT
**
** HISTORY OUTPUT: H-Output-1
**
*Output, history, variable=PRESELECT
*End Step
```